that were juxtaposed to nucleotidyl transferase domain. Finally, we narrowed the N-terminal region that is indispensable for the nucleotidyl transferase activity and nuclear localization of PAPD7. Our results point out the possibilities that PAPD7 as well as PAPD5 has strong nucleotidyl transferase activity that is conferred by the N-terminal region and that these proteins polyadenylate different RNAs.

2. Materials and methods

2.1. Plasmid construction

The coding sequences of PAPD5 (NM_001040284) and PAPD7 (NM_006999.4) were amplified from U2OS cDNA library, and cloned into pCMV-Myc (Clontech) or pCMV-5×Myc [24]. For the cloning of N-terminally extended PAPD7, primers 5′ TTG GAA TTC ATG CAG ATC TGG GAG ACC 3′ was used to amplify from −690 ATG. To construct pCI-neo-λN, inverse PCR was performed to introduce the Kozak sequence followed by N22 peptide coding sequence between the *NheI* and *EcoRI* sites of pCI-neo (Clontech). The coding sequences of 5×Myc-PAPD5, 5×Myc-PAPD7 or 5×Myc were PCR-amplified and inserted into pCI-neo-λN. Point mutants or deletion mutants were generated by inverse PCR. Note that as the nucleotide sequence between −690 ATG to +1 ATG of PAPD7 l is highly GC-rich, PCR reactions were performed using KOD plus ver.2 (Takara) in the presence of 5% DMSO or KOD FX (Takara). PCR reactions for sequencing analyses were also performed in the presence of 5% DMSO. pFlag-CMV5/TO-BGG boxB was generated by inserting 30nt spacer sequence followed by boxB sequence after BGG stop codon. To construct pBSII-5×Flag-7SK, 7SK gene including the proximal sequence element (PSE) and the TATA box was cloned into pBSII. Fag-tag sequence was inserted into 5′ end of the 7SK-coding sequence.

2.2. Antibodies

Antibodies used in this study were the following: anti-c-Myc (9E10, Roche), anti-GAPDH (6C5, Millipore), anti-C23 (H-250, Santa Cruz). Anti-PAPD5 and anti-PAPD7 were raised against His-tagged PAPD5 (517–698 a.a; NP_001035374) and PAPD7 (308–542 a.a; NP_001165276), respectively.

2.3. siRNA

The sequence of siRNA for luciferase was previously described [24]. PAPD5 and PAPD7 siRNA consisted of 5′ r (GGACGACACUU-CAAUUAUU) d(TT) 3′and 5′ r (GAAUUACAUGAAGAAAUAU) d(TT) 3′, respectively.

2.4. Cell culture and transfection

HeLa and U2OS cells were cultured in Dulbecco's modified Eagle's medium (Nissui) supplemented with 5% fetal bovine serum. Transfection of plasmid DNA was performed using Lipofectamine 2000 (Invitrogen) as described previously [25]. For siRNA transfection, Lipofectamine RNAi MAX (Invitrogen) was used.

2.5. Northern analysis

The northern blotting analysis was performed as described previously [24].

2.6. Immunolocalization analysis

Localization of PAPD5, PAPD7 and PAPD7 mutants were visualized in HeLa cells. Twenty-four hours after transfection, cells were washed once with PBS, fixed with 4% paraformaldehyde in PBS for 12 min, quenched with 10 mM Glycine in PBS for 10 min, permiabilized with 0.1% Triton X-100, 1% goat serum in PBS for 12 min, and incubated at 4 °C overnight with primary mouse anti-Myc (1:400) and rabbit anti-C23 (1:100) antibodies. Cells were then washed three times with PBS for 10 min and incubated with Alexa Fluor 488 goat anti-mouse antibody (1:200), Alexa Fluor 568 anti-rabbit antibody (1:200) and DAPI. Images were obtained using an OLYMPUS IX71 fluorescent microscope.

2.7. Accession number

The nucleotide and deduced amino acid sequence of PAPD7 l are available at GenBank (accession number KC424495).

3. Results

3.1. Identification of N-terminaly extended PAPD7 isoform

It has already been shown that PAPD5 catalyzes polyadenylation of RNA substrates *in vitro* [23]. As PAPD7 deposited in NCBI protein database shares strong identity with PAPD5 (>77%) especially in the nucleotidyl transferase domain (>92%) and PAP-associated domain (>94%), we first examined the nucleotidyl transferase activity of PAPD7 as well as PAPD5 by using MS2-based tethering strategy. HeLa cells were co-transfected with β-globin (BGG) MS2-bs reporter gene and a plasmid expressing MS2-fused PAPD5 or PAPD7. Unexpectedly, we could not detect any significant activity for PAPD7, which is in sharp contrast to PAPD5 (data not shown). Therefore, PAPD7-specific antibodies were generated in two individual rabbits using recombinant PAPD7 (C-terminal 235 a.a. of NP_001165276) prepared from *E.coli* as antigen (Fig. 1A). Western blot analysis of HeLa or U2OS cell extracts revealed that proteins commonly detected by these antibodies migrated at about 94 kDa, which was slower than the NCBI's Entrez protein (NP_001165276) migrated at about 62 kDa on SDS–PAGE (Fig. 1B and data not shown). Since 94 kDa protein was specifically depleted by treatment with siRNA against PAPD7, the NP_001165276 clone is unlikely to contain full-length PAPD7. Computational analysis of the 5′-flanking region of PAPD7 gene coding for the NCBI's Entrez mRNA (NM_006999) revealed that it has a candidate AUG triplet corresponding to the size of the 94 kDa form of PAPD7 (Supplementary Figure, positions −690 of the proposed AUG (+1)). To determine whether the upstream AUG is actually transcribed and used as the translation initiation site to produce full-length PAPD7, a primer was designed to amplify cDNA starting from the putative initiation site. The primer −690 ATG successfully amplified PAPD7 cDNA with extended 5′ sequence from a U2OS cDNA library. It is note that this PCR product was not amplified from contaminated genomic DNA as an isolated amplicon contains exon-exon junctions. To test if PAPD7 cDNA with the extended 5′ sequence indeed encodes 94 kDa form of PAPD7, this amplicon was cloned into pCMV-Myc and expressed exogenously in HeLa cells. Western blot analysis using anti-PAPD7 antibody showed that the exogenously expressed protein migrated at a similar position to endogenous PAPD7 (Fig. 1C). From these results, we conclude that the 94 kDa form of PAPD7 (hereafter referred to as PAPD7 l) has N-terminal extension compared to the NCBI's Entrez protein NP_001165276 (hereafter referred to as PAPD7 s).

Thus, we next examined nucleotidyl transferase activity of the newly identified PAPD7 l by using λN-boxB-based tethering system. The assay was performed by co-transfecting with β-globin

Please cite this article in press as: K. Ogami et al., Molecular cloning and characterization of a novel isoform of the non-canonical poly(A) polymerase PAPD7, Biochem. Biophys. Res. Commun. (2013), http://dx.doi.org/10.1016/j.bbrc.2013.01.072

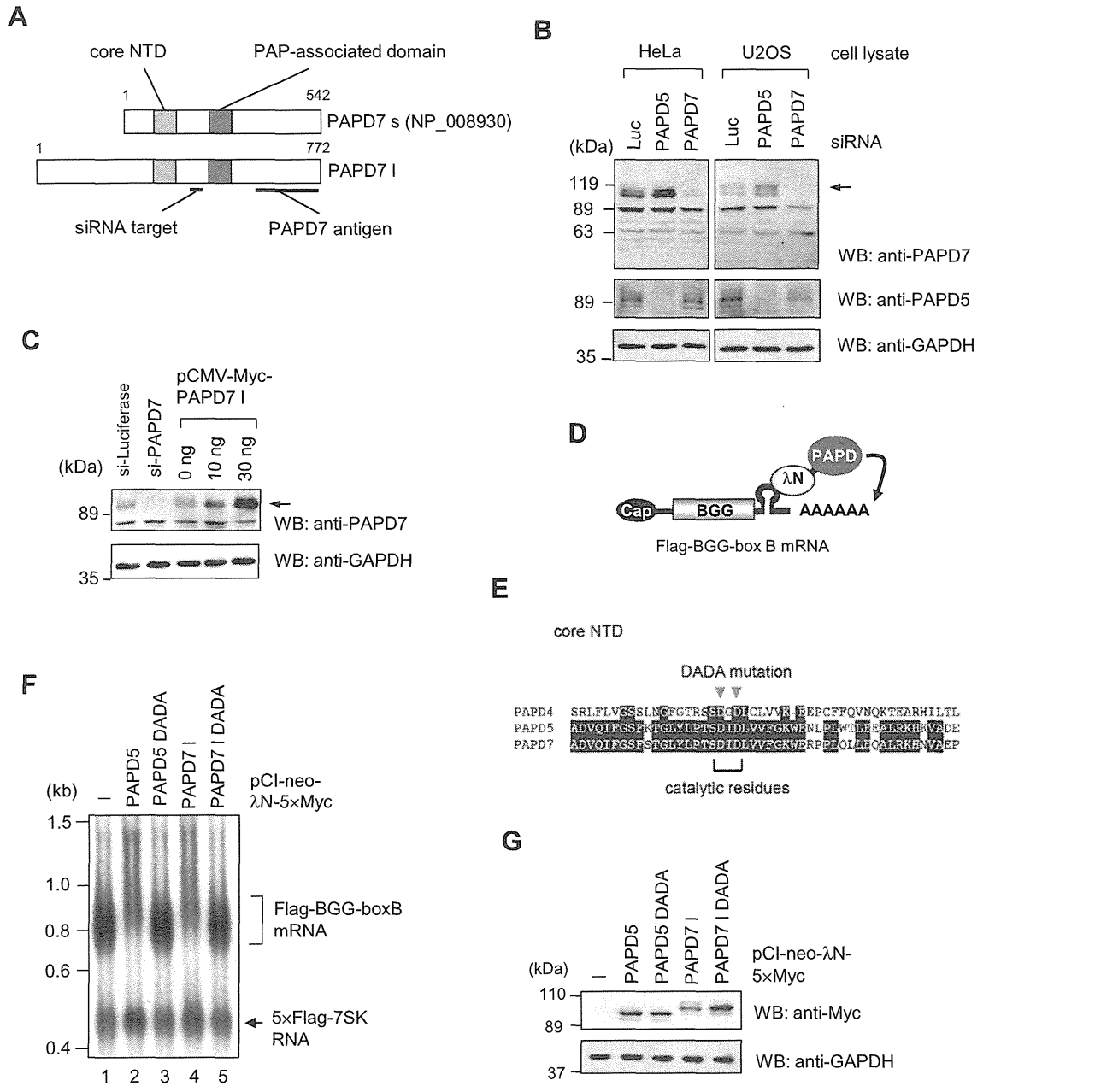

Fig. 1. Identification of 94 kDa PAPD7 isoform. (A) Scheme of original PAPD7 clone (NP_008930.1). The light- and dark-gray boxes indicate core NTD and PAP-associated domain, respectively. The areas used for antibody production and siRNA knockdown are underlined. (B) HeLa or U2OS cells were transfected with PAPD5, PAPD7 or control Luciferase siRNA for 72 h. Cell lysates were analyzed by western blotting using the indicated antibodies. An arrow indicates the protein specifically depleted by si-PAPD7.(C) HeLa cells were transfected with siRNA against PAPD7 or control Luciferase, or increasing amount of pCMV-Myc-PAPD7. Exogeous PAPD7 protein migrated at almost the same position to endogenous PAPD7 on SDS–PAGE. (D) Tethered function assays using λN-boxB-based tethering system. λN-fused PAPD proteins were brought to 3′UTR of a BGG boxB reporter mRNA, and the nucleotidyl transferase activity was examined. (E) Sequence alignment of the core nucleotidyl transferase domain of PAPD4, PAPD5 and PAPD7. Identical residues are *shaded* in *black*. (F) HeLa cells were transfected with pFlag-CMV5/TO-BGG boxB reporter plasmid, pBSII-5×Flag-7SK reference plasmid, and either pCI-neo-λN-5×Myc-PAPD5, pCI-neo-λN-5×Myc-PAPD7, or their DADA mutants. Total RNAs were prepared from the cells and subjected to northern blotting. (G) Total cell lysates were analyzed by western blotting using the indicated antibodies.

(BGG) boxB reporter and a plasmid encoding either λN-fused test protein or its mutated form (DADA) (Fig. 1D and E). Multiple Flag-tagged 7SK RNA served as transfection/loading control. When PAPD7 l was tethered to the mRNA 3′UTR, the protein displayed strong nucleotidyl transferase activity, which was comparable to that of PAPD5 (Fig. 1F, lanes 2 and 4). Mutations of two aspertate residues in the nucleotidyl transferase domain (DADA) completely abolished the nucleotidyl transferase activity of these proteins (lanes 3 and 5). The expression level of tethered proteins was confirmed by western blotting (Fig. 1G). The same result was obtained when MS2-based tethering system was used instead of λN-boxB system (data not shown).

3.2. Differential subcellular localization of PAPD5 and PAPD7

We next examined the subcellular localization of PAPD5 and PAPD7. N-terminally Myc-tagged proteins were visualized in transiently transfected HeLa cells. To discriminate between the nucleolar and nonnucleolar part, we stained nucleolar part with anti-nucleolin antibody (NCL). As previously described [21,23],

Please cite this article in press as: K. Ogami et al., Molecular cloning and characterization of a novel isoform of the non-canonical poly(A) polymerase PAPD7, Biochem. Biophys. Res. Commun. (2013), http://dx.doi.org/10.1016/j.bbrc.2013.01.072

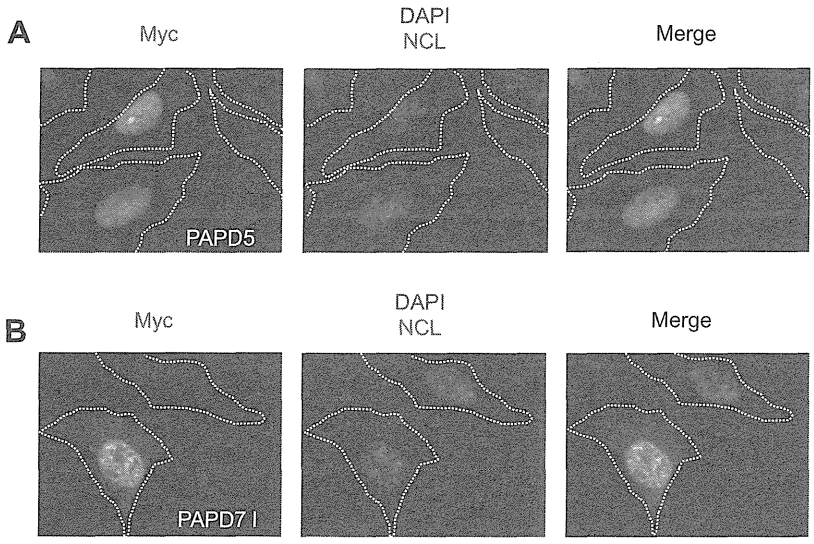

Fig. 2. Different subcellular localization of PAPD5 and PAPD7. HeLa cells were transfected with pCMV-Myc-PAPD5 (A) or pCMV-Myc-PAPD7 l (B), and the localization of expressed proteins were analyzed by immunofluorescence using anti-Myc antibody and visualized by fluorescent microscopy (green). Nucleolin (NCL) staining (red) served as a nucleolar marker and was overlaid with labeling of nuclei by DAPI (blue).

PAPD5 localized strictly to the nucleus with nucleolar accumulation as judged by the co-localization with nucleolin (Fig. 2A). PAPD7 mainly localized to the nucleus, however, in sharp contrast to PAPD5, it was excluded from the nucleolus and weak staining was detected in the cytoplasm (Fig. 2B). Similar results were obtained for U2OS cells (data not shown). These results suggest that in contrast to PAPD5, which functions in the nucleus, PAPD7 functions mainly in the nucloplasm, and also has roles in the cytoplasm.

3.3. Newly identified N-terminal region is indispensable for both the nucleotidyl transferase activity and the nuclear localization of PAPD7

As described above, we have observed that tethering of PAPD7 l but not PAPD7 s that lacks N-terminal region (NP_001165276) results in extensive nucleotide transfer to mRNA substrates (Fig. 3B, PAPD7 l and s). These facts imply that there is a region that is indispensable for catalytic activity of PAPD7 in the newly identified N-terminal region, besides the nucleotidyl transferase domain and PAP-associated domain. To search for such a region, we first compared the N-terminal sequence of PAPD7 l with its corresponding region of PAPD5 and identified a highly conserved sequence that is located in juxtaposition to nucleotidyl transferase domain (Fig. 3A). The sequence identified is absent in other non-canonical poly(A) polymerases. Deletion of this region completely abolished the nucleotidyl transferase activity of PAPD7 (Fig. 3B, Δ1). To further narrow the area, we prepared a set of deletion constructs (Fig. 3A, Δ2–Δ4). PAPD7 residues 167–186 which contain a stretch of basic amino acids are dispensable for the nucleotidyl transferase activity (Fig. 3A and B, Δ2). In contrast, PAPD7 lacking residues 187–230 did not show nucleotidyl transferase activity (Δ3). The Δ4 mutant that lacks residues 187–219 but contains residues 220–230 which are conserved in PAPD5 and yeast Trf4 protein was not able to transfer nucleotides to the reporter mRNA. The expression level of tethered proteins was confirmed by western blotting (Fig. 3C). Taken together, we conclude that not only core NTD but also residues 187–219 are required for the full nucleotidyl transferase activity of PAPD7.

In addition to the difference in the nucleotidyl transferase activity between PAPD7 l and PAPD7 s, we found that these proteins exhibit different distribution in cells (Fig. 3D and E). PAPD7 l was more abundant in the nucleus than the cytoplasm, whereas PAPD7 s that lacks N-terminal residues evenly distributed throughout the cell. To investigate the region responsible for the nuclear localization of PAPD7 l, we utilized the deletion mutants (Δ1–Δ4). Unexpectedly, the same distribution as PAPD7 l was observed only in Δ2 mutant, although the mutant lacks a putative nuclear localization signal (NLS)-like sequence (RRKR). In contrast, other mutants showed strong cytoplasmic localization (Δ1, Δ3 and Δ4), indicating that PAPD7 residues 187–219 are required for the nuclear localization of PAPD7.

4. Discussion

In this report, we have identified a novel N-terminally extended 94 kDa isoform of PAPD7 (PAPD7 l). Translation of this isoform starts at AUG codon located at 690 nt upstream from the previously predicted start codon of NCBI's Entrez mRNA (NM_006999) which encodes 62 kDa isoform of PAPD7 (PAPD7 s). Interestingly, the PAPD7 l but not PAPD7 s exhibits nucleotidyl transferase activity. This finding and the fact that only 94 kDa protein was specifically depleted by siRNA against PAPD7 in both HeLa and U2OS cells indicate that the PAPD7 l is the major and active isoform that is actually expressed in cells.

The observation that PAPD7 l but not PAPD7 s showed catalytic activity was surprising, because both isoforms contain nucleotidyl transferase domain. Analysis of deletion mutants revealed the importance of residues 187–219 for the nucleotidyl transferase activity of PAPD7 l. This region is also required for nuclear localization of PAPD7 l. It appears that nuclear retention of PAPD7 l correlates with the nucleotidyl transferase activity; the deletion mutants that lost its catalytic activity have a tendency to localize in the cytoplasm. Since no putative NLS was found in this region, we hypothesize that this region is involved in the interaction with other factors that is required for nuclear retention and the nucleotidyl transferase activity of PAPD7 l.

While PAPD7 l lacking residues 167–230 (Δ1) is almost exclusively cytoplasmic, PAPD7 l lacking residues 1–230 (PAPD7 s) is evenly distributed throughout the cell. These results led us to speculate that PAPD7 l contains a nuclear export signal (NES) in residues 1–166. We therefore treated cells with a nuclear export inhibitor, leptomycin B (LMB) and examined subcellular

Please cite this article in press as: K. Ogami et al., Molecular cloning and characterization of a novel isoform of the non-canonical poly(A) polymerase PAPD7, Biochem. Biophys. Res. Commun. (2013), http://dx.doi.org/10.1016/j.bbrc.2013.01.072

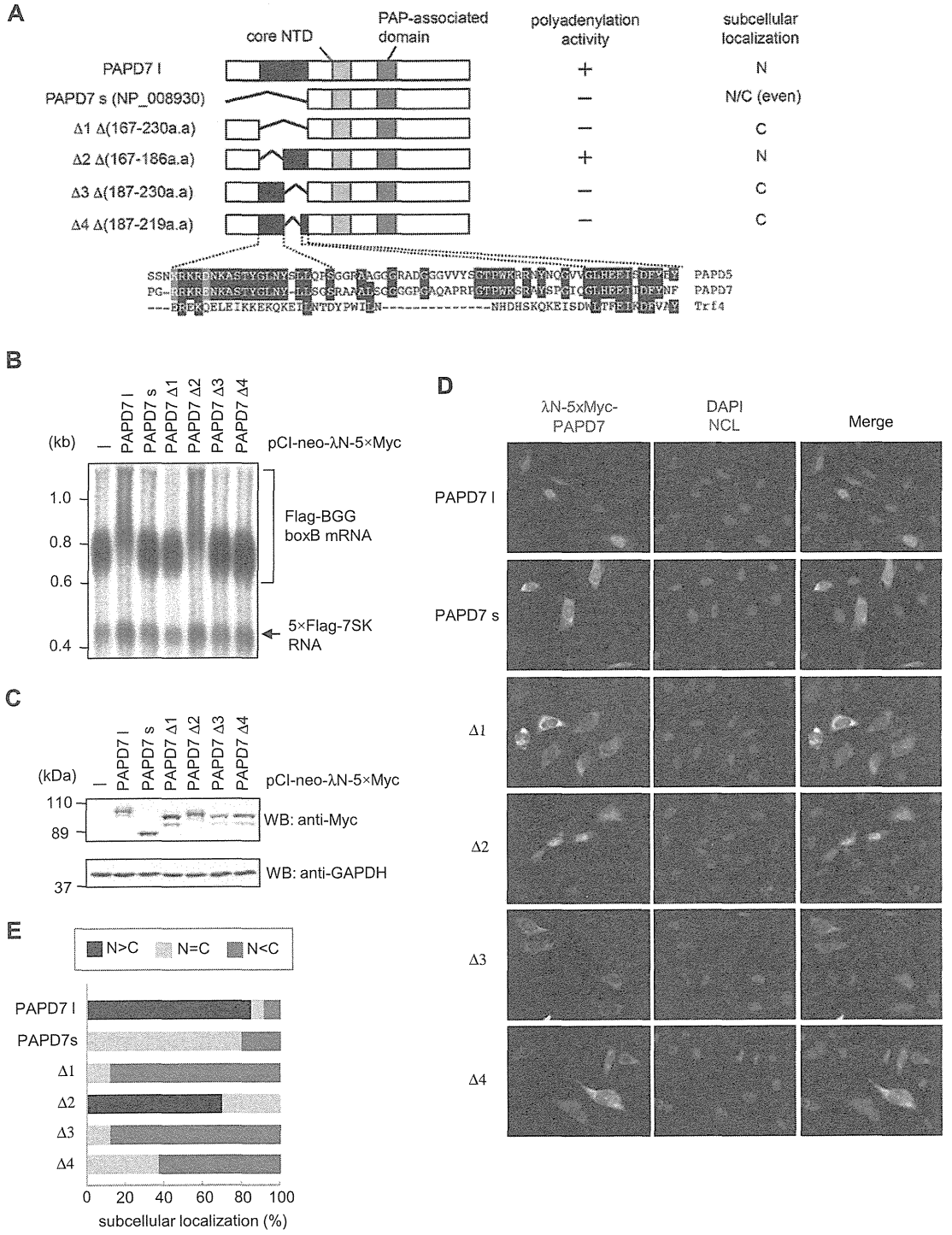

Fig. 3. Identification of an N-terminal region that is indispensable for both the nucleotidyl transferase activity and nuclear localization. (A) Overview of mutant forms of PAPD7 proteins used in this study. The core nucleotidyl transferase domain (core NTD) and PAP-associated domain are indicated by the light and dark gray boxes, respectively. The black box indicates the region that is conserved between PAPD5 and PAPD7, and its sequence alignments were shown below. The summary of the nucleotidyl transferase activity and the subcellular localization of these proteins are shown on the right. (B) HeLa cells were transfected with pFlag-CMV5/TO-BGG boxB reporter plasmid, pBSII-5×Flag-7SK reference plasmid, and either pCI-neo-λN-5×Myc-PAPD7 or its deletion mutants. Total RNAs were prepared from the cells and subjected to northern blotting. (C) Total cell lysates were analyzed by western blotting using indicated antibodies. (D) HeLa cells were transfected with pCI-neo-λN-5×Myc-PAPD7 or its deletion mutants and the localization of expressed proteins were analyzed by immunofluorescence using anti-Myc antibody and visualized by fluorescent microscopy (green). Nucleolin (NCL) staining (red) served as a nucleolar marker and was overlaid with labeling of nuclei by DAPI (blue). (E) Histogram showing the intracellular distribution of each construct. Shown is the proportion in each compartment, using measurements from 48–71 cells for each construct.

localization of Δ1 mutant. However, LMB treatment did not cause nuclear accumulation of the mutant: Δ1 mutant remain cytoplasmic after the incubation with LMB (data not shown). Thus, it is unlikely that the cytoplasmic localization of PAPD7 mutants is the result of Crm1-dependent nuclear export.

An interesting and important observation is that PAPD7 and its paralog PAPD5 display different intracellular distributions. PAPD5, in agreement with previously published results, is restricted to the nucleus with nucleolar enrichment [21]. In contrast, the majority of PAPD7 is nuclear but excluded from nucleoli. We also confirmed

Please cite this article in press as: K. Ogami et al., Molecular cloning and characterization of a novel isoform of the non-canonical poly(A) polymerase PAPD7, Biochem. Biophys. Res. Commun. (2013), http://dx.doi.org/10.1016/j.bbrc.2013.01.072

a minor cytoplasmic pool of PAPD7. We therefore propose that the biological functions of these paralogs are not equivalent. In support of this proposal, previous study demonstrated that PAPD5 but not PAPD7 is responsible for the polyadenylation of aberrant pre-rRNAs in mouse cells [18] and in human cells (our unpublished data). We note that despite the previous work using PAPD7 s [22], we were unable to confirm the interaction between PAPD7 and ZCCHC7 (data not shown). As ZCCHC7 was shown to display a strict nucleolar localization [21,22], and as PAPD7 s is also excluded from nucleoli, we think it is unlikely that PAPD7 forms complex with ZCCHC7. On the other hand, we could detect the interaction between PAPD5 and ZCCHC7 (as described previously [21] and data not shown) indicating that PAPD5 is truly a component of the nucleolar TRAMP-like complex in human cells.

The functional relevance of PAPD7 as well as PAPD5 outside nucleoli remains to be elucidated, however, several evidences point out the possibility that PAPD7 and/or PAPD5 are also involved in the pre-mRNA processing in the nucleoplasm. First, PAPD7 s was shown to interact with a non-nucleolar protein PRPF31 that is necessary for U4/U6•U5 tri-snRNP formation [26,27]. PAPD5 also interacts with a subset of splicing factors including PRPF31 [21]. Second, in budding yeast, the function of Trf4p is not restricted to ncRNA surveillance. It has been reported that Trf4p but not Trf5p is indispensable for the proper 3′ end formation of mRNAs encoding Nab2 [28] or Cth2 [29]. Future research will aim to identify the substantial substrate of PAPD7 and to determine whether PAPD7 and PAPD5 work redundantly or independently in the nucleoplasm.

Acknowledgments

This work was supported by a Grant-in-Aid for Scientific Research on Innovative Areas "RNA regulation" (No. 20112005) from the Ministry of Education, Culture, Sports, Science and Technology of Japan, and a Grant-in-Aid for Scientific Research (B) (No. 21370080) from Japan Society for the Promotion of Science (to S H).

Appendix A. Supplementary data

Supplementary data associated with this article can be found, in the online version, at http://dx.doi.org/10.1016/j.bbrc.2013.01.072.

References

[1] M.J. Schmidt, C.J. Norbury, Polyadenylation and beyond: emerging roles for noncanonical poly(A) polymerases, Wiley Interdiscip. Rev. RNA 1 (2010) 142–151.
[2] G. Martin, W. Keller, RNA-specific ribonucleotidyl transferases, RNA 13 (2007) 1834–1849.
[3] J. LaCava, J. Houseley, C. Saveanu, E. Petfalski, E. Thompson, A. Jacquier, D. Tollervey, RNA degradation by the exosome is promoted by a nuclear polyadenylation complex, Cell 121 (2005) 713–724.
[4] J. Houseley, D. Tollervey, Yeast Trf5p is a nuclear poly(A) polymerase, EMBO Rep. 7 (2006) 205–211.
[5] J.T. Arigo, D.E. Eyler, K.L. Carroll, J.L. Corden, Termination of cryptic unstable transcripts is directed by yeast RNA-binding proteins Nrd1 and Nab3, Mol. Cell 23 (2006) 841–851.
[6] M. Thiebaut, E. Kisseleva-Romanova, M. Rougemaille, J. Boulay, D. Libri, Transcription termination and nuclear degradation of cryptic unstable transcripts: a role for the nrd1-nab3 pathway in genome surveillance, Mol. Cell 23 (2006) 853–864.
[7] F. Wyers, M. Rougemaille, G. Badis, J.C. Rousselle, M.E. Dufour, J. Boulay, B. Regnault, F. Devaux, A. Namane, B. Seraphin, D. Libri, A. Jacquier, Cryptic pol II transcripts are degraded by a nuclear quality control pathway involving a new poly(A) polymerase, Cell 121 (2005) 725–737.
[8] C.A. Davis, M. Ares Jr., Accumulation of unstable promoter-associated transcripts upon loss of the nuclear exosome subunit Rrp6p in Saccharomyces cerevisiae, Proc. Natl. Acad. Sci. USA 103 (2006) 3262–3267.
[9] C. Dez, J. Houseley, D. Tollervey, Surveillance of nuclear-restricted pre-ribosomes within a subnucleolar region of Saccharomyces cerevisiae, EMBO J. 25 (2006) 1534–1546.
[10] D.E. Egecioglu, A.K. Henras, G.F. Chanfreau, Contributions of Trf4p- and Trf5p-dependent polyadenylation to the processing and degradative functions of the yeast nuclear exosome, RNA 12 (2006) 26–32.
[11] T. Carneiro, C. Carvalho, J. Braga, J. Rino, L. Milligan, D. Tollervey, M. Carmo-Fonseca, Depletion of the yeast nuclear exosome subunit Rrp6 results in accumulation of polyadenylated RNAs in a discrete domain within the nucleolus, Mol. Cell Biol. 27 (2007) 4157–4165.
[12] J. Houseley, K. Kotovic, A. El Hage, D. Tollervey, Trf4 targets ncRNAs from telomeric and rDNA spacer regions and functions in rDNA copy number control, EMBO J. 26 (2007) 4996–5006.
[13] S. San Paolo, S. Vanacova, L. Schenk, T. Scherrer, D. Blank, W. Keller, A.P. Gerber, Distinct roles of non-canonical poly(A) polymerases in RNA metabolism, PLoS Genet. 5 (2009) e1000555.
[14] K.P. Callahan, J.S. Butler, TRAMP complex enhances RNA degradation by the nuclear exosome component Rrp6, J. Biol. Chem. 285 (2010) 3540–3547.
[15] S. Kadaba, A. Krueger, T. Trice, A.M. Krecic, A.G. Hinnebusch, J. Anderson, Nuclear surveillance and degradation of hypomodified initiator tRNAMet in *S. cerevisiae*, Genes Dev. 18 (2004) 1227–1240.
[16] S. Vanacova, J. Wolf, G. Martin, D. Blank, S. Dettwiler, A. Friedlein, H. Langen, G. Keith, W. Keller, A new yeast poly(A) polymerase complex involved in RNA quality control, PLoS Biol. 3 (2005) e189.
[17] C. Walowsky, D.J. Fitzhugh, I.B. Castano, J.Y. Ju, N.A. Levin, M.F. Christman, The topoisomerase-related function gene TRF4 affects cellular sensitivity to the, J. Biol. Chem. 274 (1999) 7302–7308.
[18] N. Shcherbik, M. Wang, Y.R. Lapik, L. Srivastava, D.G. Pestov, Polyadenylation and degradation of incomplete RNA polymerase I transcripts in mammalian cells, EMBO Rep. 11 (2010) 106–111.
[19] T.E. Mullen, W.F. Marzluff, Degradation of histone mRNA requires oligouridylation followed by decapping and simultaneous degradation of the mRNA both 5′–3′ and 3′–5′, Genes Dev. 22 (2008) 50–65.
[20] H. Berndt, C. Harnisch, C. Rammelt, N. Stohr, A. Zirkel, J.C. Dohm, H. Himmelbauer, J.P. Tavanez, S. Huttelmaier, E. Wahle, Maturation of mammalian H/ACA box snoRNAs: PAPD5-dependent adenylation and PARN-dependent trimming, RNA 18 (2012) 958–972.
[21] M. Lubas, M.S. Christensen, M.S. Kristiansen, M. Domanski, L.G. Falkenby, S. Lykke-Andersen, J.S. Andersen, A. Dziembowski, T.H. Jensen, Interaction profiling identifies the human nuclear exosome targeting complex, Mol. Cell 43 (2011) 624–637.
[22] M.B. Fasken, S.W. Leung, A. Banerjee, M.O. Kodani, R. Chavez, E.A. Bowman, M.K. Purohit, M.E. Rubinson, E.H. Rubinson, A.H. Corbett, Air1 zinc knuckles 4 and 5 and a conserved IWRXY motif are critical for the function and integrity of the Trf4/5-Air1/2-Mtr4 polyadenylation (TRAMP) RNA quality control complex, J. Biol. Chem. 286 (2011) 37429–37445.
[23] C. Rammelt, B. Bilen, M. Zavolan, W. Keller, PAPD5, a noncanonical poly(A) polymerase with an unusual RNA-binding motif, RNA 17 (2011) 1737–1746.
[24] N. Hosoda, Y. Funakoshi, M. Hirasawa, R. Yamagishi, Y. Asano, R. Miyagawa, K. Ogami, M. Tsujimoto, S. Hoshino, Anti-proliferative protein Tob negatively regulates CPEB3 target by recruiting Caf1 deadenylase, EMBO J. 30 (2011) 1311–1323.
[25] Y. Funakoshi, Y. Doi, N. Hosoda, N. Uchida, M. Osawa, I. Shimada, M. Tsujimoto, T. Suzuki, T. Katada, S. Hoshino, Mechanism of mRNA deadenylation: evidence for a molecular interplay between translation termination factor eRF3 and mRNA deadenylases, Genes Dev. 21 (2007) 3135–3148.
[26] A. Nag, J.A. Steitz, Tri-snRNP-associated proteins interact with subunits of the TRAMP and nuclear, RNA Biol. 9 (2012) 334–342.
[27] O.V. Makarova, E.M. Makarov, S. Liu, H.P. Vornlocher, R. Luhrmann, Protein 61K, encoded by a gene (PRPF31) linked to autosomal dominant retinitis, EMBO J. 21 (2002) 1148–1157.
[28] K.M. Roth, J. Byam, F. Fang, J.S. Butler, Regulation of NAB2 mRNA 3'-end formation requires the core exosome and the Trf4p component of the TRAMP complex, RNA 15 (2009) 1045–1058.
[29] D. Ciais, M.T. Bohnsack, D. Tollervey, The mRNA encoding the yeast ARE-binding protein Cth2 is generated by a novel 3′ processing pathway, Nucleic Acids Res. 36 (2008) 3075–3084.

Please cite this article in press as: K. Ogami et al., Molecular cloning and characterization of a novel isoform of the non-canonical poly(A) polymerase PAPD7, Biochem. Biophys. Res. Commun. (2013), http://dx.doi.org/10.1016/j.bbrc.2013.01.072

Oncogene (2012), 1–10

www.nature.com/onc

ORIGINAL ARTICLE

Antiproliferative protein Tob directly regulates c-myc proto-oncogene expression through cytoplasmic polyadenylation element-binding protein CPEB

K Ogami, N Hosoda, Y Funakoshi and S Hoshino

The regulation of mRNA deadenylation constitutes a pivotal mechanism of the post-transcriptional control of gene expression. Here we show that the antiproliferative protein Tob, a component of the Caf1–Ccr4 deadenylase complex, is involved in regulating the expression of the proto-oncogene c-myc. The c-myc mRNA contains *cis* elements (CPEs) in its 3′-untranslated region (3′-UTR), which are recognized by the cytoplasmic polyadenylation element-binding protein (CPEB). CPEB recruits Caf1 deadenylase through interaction with Tob to form a ternary complex, CPEB–Tob–Caf1, and negatively regulates the expression of c-myc by accelerating the deadenylation and decay of its mRNA. In quiescent cells, c-myc mRNA is destabilized by the *trans*-acting complex (CPEB–Tob–Caf1), while in cells stimulated by the serum, both Tob and Caf1 are released from CPEB, and c-Myc expression is induced early after stimulation by the stabilization of its mRNA as an 'immediate-early gene'. Collectively, these results indicate that Tob is a key factor in the regulation of c-myc gene expression, which is essential for cell growth. Thus, Tob appears to function in the control of cell growth at least, in part, by regulating the expression of c-myc.

Oncogene advance online publication, 26 November 2012; doi:10.1038/onc.2012.548

Keywords: Tob; Caf1; CPEB; mRNA decay; deadenylation

INTRODUCTION

In eukaryotes, the mRNA poly(A) tail has pivotal roles in the post-transcriptional control of gene expression. The 3′ poly(A) tail interacts with the 5′ cap to circularize mRNA, which leads to a synergistic activation of translation.[1,2] Also, shortening of the poly(A) tail, termed deadenylation, is the rate-limiting step in general mRNA decay.[3] Thus, the regulation of the poly(A) tail length contributes greatly to the control of gene expression in terms of both translation and mRNA stability.[4,5] Especially in oocyte maturation and early embryonic development, which occur in the absence of transcription, gene expression is absolutely regulated by the polyadenylation and deadenylation of maternal mRNA. In this case, CPE-containing pre-mRNA such as cyclin B1 acquires a long poly(A) tail in the nucleus that is subsequently shortened when transported to the cytoplasm. The poly(A) tail length is controlled by two cytoplasmic polyadenylation element-binding protein (CPEB)-associated proteins: a poly(A)-specific ribonuclease (PARN) deadenylase[6] and a poly(A) polymerase Gld2.[7] CPEB recruits PARN to the CPE-containing mRNA and accelerates the deadenylation reaction. Upon oocyte maturation, CPEB phosphorylation leads to the dissociation of PARN from the RNP complex and instead Gld2 associated with CPEB catalyzes default polyadenylation.[8] Thus, cytoplasmic polyadenylation activates the translation of specific mRNAs.

In somatic cells, however, poly(A) tail length is regulated mostly by deadenylation that is generally catalyzed by two major mRNA deadenylase complexes, Pan2–Pan3 and Caf1–Ccr4.[9] The former consists of the catalytic subunit Pan2 and regulatory subunit Pan3.[10] Pan3 binds to the poly(A)-binding protein PABPC1 by using the PAM2 motif and makes Pan2 accessible to the substrate poly(A), which leads to the activation of deadenylation.[10] On the other hand, both the Caf1 and Ccr4 subunits of the latter complex have the catalytic activities of the deadenylase.[11–13] The antiproliferative protein Tob forms a complex with Caf1–Ccr4[14] and mediates the binding of the deadenylases to PABPC1.[15] As in the case of Pan3, Tob binds to PABPC1 via the PAM2 motif and makes Caf1–Ccr4 accessible to the PABPC1-bound poly(A), which also leads to the activation of deadenylation.[16,17] We have previously found that the termination of translation triggers mRNA deadenylation, and proposed an initiation mechanism of mRNA decay: after translation termination, the termination complex eRF1–eRF3 is released from PABPC1, and in turn the two deadenylase complexes, Pan2–Pan3 and Caf1–Ccr4, bind to PABPC1 to degrade the poly(A) tail of the mRNA.[17] The translation termination factor eRF3 also contains PAM2 motifs, and competition between eRF3 and the two deadenylase complexes for the binding of PABPC1 is the key to this model.[17,18]

In addition to the decay of general mRNA, Tob in a complex with Caf1 also has an important role in the regulation of specific mRNA. Tob binds directly to a sequence-specific RNA-binding protein, CPEB3, and recruits Caf1 to the target of CPEB3.[19] The binding of CPEB3 to the target, AMPA receptor (GluR2) mRNA, leads to accelerated deadenylation and decay of the message and inhibition of its expression. Thus, Tob is thought to function in learning and memory by regulating the expression of the AMPA receptor.[19]

Tob is a multifunctional protein involved not only in learning and memory[20,21] but also in cell cycle progression,[22,23] spermatogenesis,[24] embryonic development,[25] osteogenesis[26]

Department of Biological Chemistry, Graduate School of Pharmaceutical Sciences, Nagoya City University, Nagoya, Japan. Correspondence: Professor S Hoshino, Department of Biological Chemistry, Graduate School of Pharmaceutical Sciences, Nagoya City University, 3-1 Tanabe-dori, Mizuho-ku, Nagoya 467-8603, Japan.
E-mail: hoshino@phar.nagoya-cu.ac.jp.
Received 1 May 2012; revised 21 September 2012; accepted 28 September 2012

and T-cell activation.[27] Among its known biological functions, Tob's role as a negative regulator of the cell cycle is well established. Ectopic expression of Tob or its paralog Tob2 results in the inhibition of cell proliferation.[14,22,23] Tob suppresses cyclin D1 expression upstream of Rb phosphorylation and inhibits G1-to-S phase transition.[23] However, the role of Tob in mRNA deadenylation with respect to cell growth regulation remains to be determined.

Here, we show that Tob directly regulates c-myc oncogene expression during G1-to-S phase transition. In quiescent cells, Tob forms a ternary complex CPEB–Tob–Caf1 and recruits Caf1 deadenylase to the target c-myc mRNA to degrade rapidly the message. After serum stimulation, Tob and Caf1 dissociate from CPEB, which leads to the stabilization of the mRNA and activation of its gene expression. Thus, Tob appears to function in the control of cell growth at least, in part, by regulating the expression of c-myc.

RESULTS

Tob directly binds CPEB to form a ternary complex with Caf1 deadenylase

We have previously shown that Tob directly binds to form a complex with the sequence-specific RNA-binding proteins CPEB3 and CPEB4.[19] Detailed analysis of the interaction revealed that Tob binds to the carboxyl-terminal RNA-binding domain of CPEB3/4. Since the RNA-binding domain is highly conserved among CPEB2–4 (>95% identity), and distantly related CPEB still has a homologous domain (~40–50% identity), we speculated that Tob also binds to CPEB. Thus, we first examined the interaction with a glutathione *S*-transferase (GST) pull-down assay. GST-Tob (1–285) and MBP-CPEB, which had been prepared from *Escherichia coli* with >95% purity, were mixed and pulled down by glutathione sepharose beads. Western blot analysis with anti-MBP antibody revealed the presence of MBP-CPEB, while it was not detected in the control experiment with GST (Figure 1a). The interaction was further confirmed with co-immunoprecipitation experiment. When lysate of HeLa cells expressing 5 × Flag-CPEB, 5 × Myc-Tob and 5 × Myc-Caf1 was immunoprecipitated with anti-Flag antibody, the precipitated fraction contained 5 × Myc-Tob (Figure 1b). Also, we have confirmed the presence of 5 × Myc-Caf1 in the precipitate. The precipitated amount of 5 × Myc-Caf1 was increased when 5 × Myc-Tob was expressed (Figure 1b, compare lanes 5 and 6). These interactions seemed not to be mediated by RNA since the binding experiments were performed in the presence of RNase A. These results indicate that Tob directly binds CPEB, as in the case of CPEB3 and CPEB4, to form a ternary complex with Caf1 deadenylase.

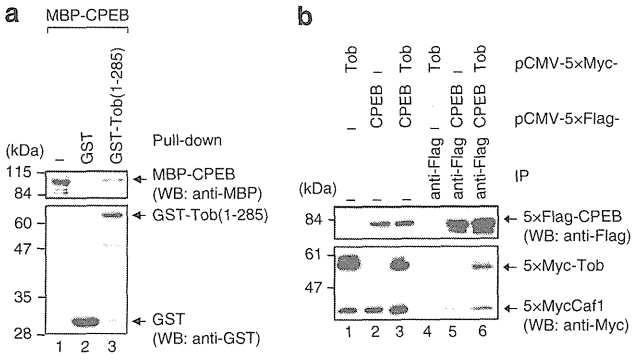

Figure 1. Tob directly binds CPEB to form a ternary complex with Caf1 deadenylase. (**a**) GST or GST-Tob was immobilized on glutathione sepharose resin and incubated with MBP-CPEB. The bound proteins (lanes 2 and 3) and the input (lane 1) were analyzed by western blotting (WB) with the indicated antibodies. (**b**) HeLa cells were transfected with pCMV-5 × Myc-Caf1, pCMV-5 × Myc-Tob, and either pCMV-5 × Flag-CPEB or pCMV-5 × Flag. The cell extracts were subjected to immunoprecipitation (IP) using anti-Flag antibody in the presence of RNase A. The immunoprecipitates (lanes 4–6) and inputs (lanes 1–3) were analyzed by western blotting with the indicated antibodies.

CPEB represses expression of c-myc 3′-UTR reporter gene by destabilizing its mRNA

The observed interaction between CPEB, Tob and Caf1 led us to speculate that CPEB's target mRNAs are regulated by deadenylation. Previous study has shown that c-myc mRNA, which contains CPEs and CPE-like sequences in its 3′-UTR (Figure 2a), is one of the targets of CPEB.[28] In an attempt to determine the significance of the interaction between CPEB, Tob and Caf1, a *β-globin* gene (BGG) reporter appended with the c-myc 3′-UTR (c-myc 3′-UTR reporter) was constructed, and the effect of CPEB on the expression of the reporter was examined by western and northern blot analyses. Exogenously expressed CPEB significantly lowered the level of BGG reporter protein in a dose-dependent manner (Figures 2b and d). This result seems not merely to be a consequence of translational repression because CPEB also reduces the level of the reporter mRNA (Figures 2c and e). The steady-state level of the reporter mRNA was reduced to ~30% by CPEB (Figure 2e), where that of the protein was reduced to ~5% (Figure 2d), suggesting that CPEB negatively regulates the reporter gene expression also at the mRNA level. The ability of CPEB to reduce the reporter mRNA and protein expression is dependent on its binding to the mRNA, as CPEB did not significantly affect the expression of the reporter gene with mutated CPEs (Figures 2b and c, lanes 4–6).

To determine whether CPEB reduces the c-myc mRNA level by promoting mRNA decay, we conducted a transcriptional pulse-chase analysis by using Tet-on system (Figure 2f). The BGG with the c-myc 3′-UTR (c-myc 3′-UTR reporter) was placed under the control of the 'Tet-on' promoter. Transcription was allowed to proceed for 2 h by adding tetracycline in T-REx HeLa cells. Cells were then washed three times to block further transcription, and total RNA was prepared from the cells sequentially after transcription was shut off. Northern blot analysis showed that the stability of c-myc 3′-UTR reporter mRNA was decreased approximately twofold by the presence of CPEB (Figures 2f and g). The signal intensity of the band was quantified along the length of the mRNA and plotted as a function of mRNA size (Figure 2h). The position of the fully deadenylated RNA (A_0) was determined by treating the steady-state mRNA with oligo (dT)/RNase H. The c-myc 3′-UTR mRNA was gradually shortened (Figure 2h, upper panel), while in cells expressing CPEB, the mRNA migrates faster to the A_0 position (Figure 2h, middle panel). The observed size difference is due to the difference in the length of the poly(A) tails, as the mRNAs were converged to the A_0 position by oligo(dT)/ RNase H treatment (Supplementary Figure S1). From these results, we conclude that CPEB accelerates deadenylation and decay of c-myc mRNA. We note that these results are not due to a secondary or nonspecific effect of CPEB, as CPEB alone did not accelerate the decay of a reporter mRNA appended with MS2-binding sites in its 3′-UTR but without CPEs (Supplementary Figure S2). On the other hand, MS2-CPEB increased the rate of deadenylation and decay for the reporter mRNA (Supplementary Figure S2). These observations further confirm that CPEB promotes deadenylation and decay of c-myc mRNA through its binding to the 3′-UTR.

Caf1 is responsible for the CPEB-accelerated decay of c-myc 3′-UTR mRNA

Next, we sought to determine whether the CPEB-accelerated decay of c-myc 3′-UTR reporter mRNA was mediated by Caf1 deadenylase. For this purpose, we applied a dominant-negative

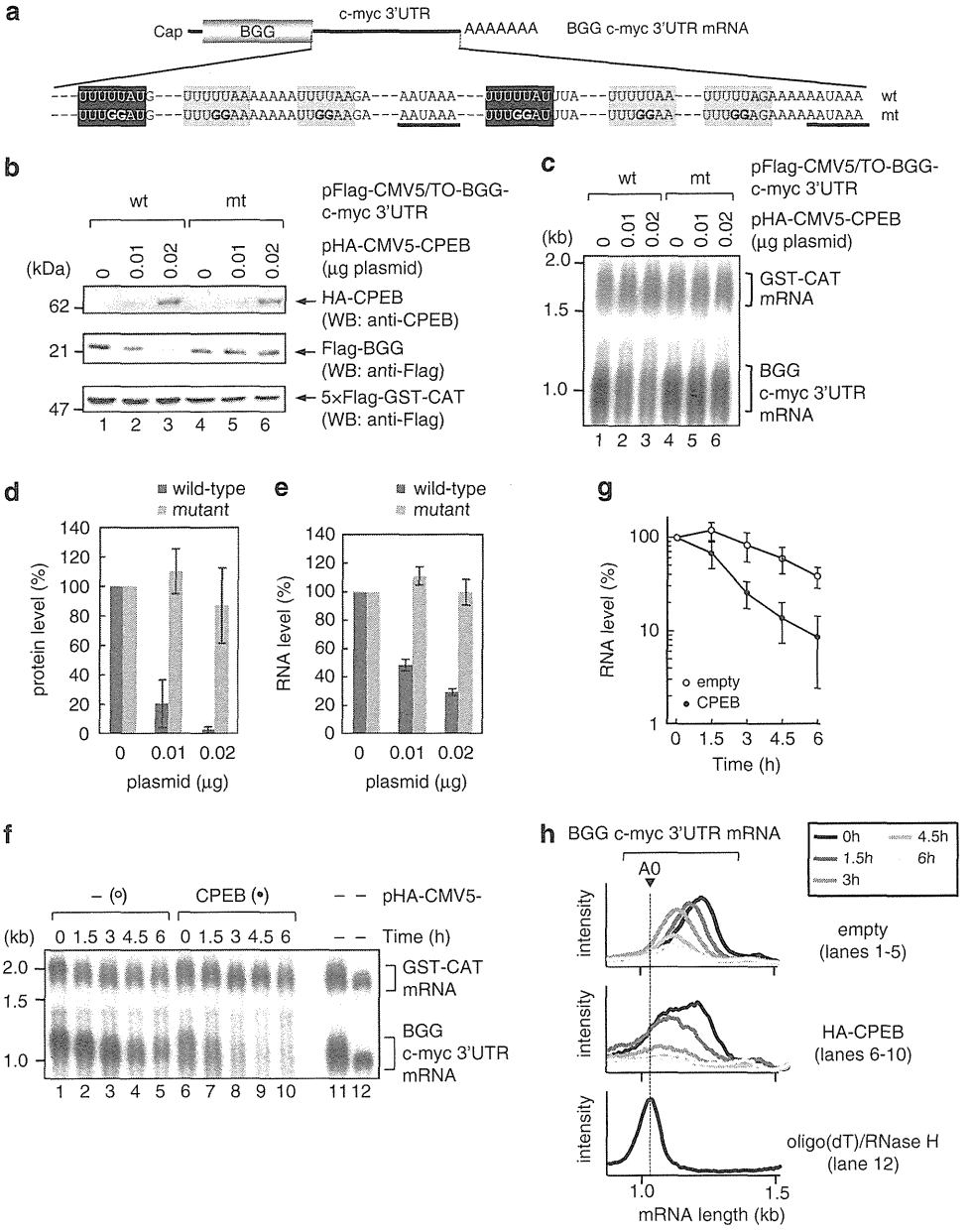

Figure 2. CPEB negatively regulates the expression of c-myc 3′-UTR reporter by promoting mRNA decay. (**a**) Schematic diagram of c-myc 3′-UTR reporter mRNA. Open reading frame of the BGG mRNA was appended with the human c-myc 3′-UTR, which contains two consensus CPEs (black box), four non-consensus CPEs (gray box) and two polyadenylation hexanucleotide sequences (black line). Bold letters designate nucleotides that were changed in the mutant reporter. (**b**) HeLa cells were transfected with increasing amounts of pHA-CMV5-CPEB, a reference plasmid pCMV-5 × Flag-GST-CAT, and either pFlag-CMV5/TO-BGG c-myc 3′-UTR (lanes 1–3) or pFlag-CMV5/TO-BGG c-myc 3′-UTR mutant (lanes 4–6). The cell extracts were subjected to western blotting (WB) with the indicated antibodies. 5 × Flag-GST-CAT served as a transfection/loading control. (**c**) HeLa cells were transfected as in (**b**). Total RNA was prepared from the cells and subjected to northern blotting. (**d**) The amount of BGG protein as in (**b**) was measured and normalized by GST-CAT protein. The score without pHA-CMV5-CPEB was defined as 100%. Data are the mean ± s.d. ($n = 3$). (**e**) The amount of BGG c-myc 3′-UTR mRNA as in (**c**) was measured and normalized by GST-CAT mRNA. The score without pHA-CMV5-CPEB was defined as 100%. Data are the mean ± s.d. ($n = 3$). (**f**) T-REx HeLa cells were co-transfected with the pFlag-CMV5/TO-BGG c-myc 3′-UTR reporter plasmid, a reference plasmid pCMV-5 × Flag-GST-CAT, and either pHA-CMV5 (lanes 1–5) or pHA-CMV5-CPEB (lanes 6–10). After 1 day, BGG mRNA was induced to express by treatment with tetracycline for 2 h, and cells were harvested at the specified time after the transcription was shut off. To analyze steady-state mRNAs, BGG mRNA was induced to express by treatment with tetracycline for 16 h (lane 11). The steady-state mRNAs were digested with *RNase*H in the presence of oligo (dT) to mark the deadenylated mRNAs (lane 12). (**g**) The level of BGG c-myc 3′-UTR mRNA as in (**f**) was quantified and normalized by the level of GST-CAT mRNA. The score from the 0 h time point was defined as 100%. Data are the mean ± s.d. ($n = 3$). (**h**) BGG c-myc 3′-UTR mRNA distribution was visualized by quantifying the signal intensity from northern blot in (**f**).

approach. T-REx HeLa cells were co-transfected with the c-myc 3′-UTR plasmid and a plasmid expressing CPEB, with or without a plasmid expressing a nuclease-deficient Caf1 mutant in which a catalytically essential aspartate residue was mutated to alanine (Caf1 D161A), and a transcriptional pulse-chase analysis was performed. The Caf1 mutant almost completely blocked CPEB-accelerated deadenylation and decay of the c-myc 3′-UTR reporter mRNA (Figures 3a and b). In contrast, a Pan2 mutant

(Pan2 D1083A) that had no deadenylase activity showed no apparent effect. The expression of comparable amounts of Caf1 D161A and Pan2 D1083A was confirmed by western blotting (Figure 3e).

In this relation, CPEB is known to bind another deadenylase PARN to regulate deadenylation of its target mRNA in the *Xenopus* oocyte.[8] The interaction was recapitulated between human-derived CPEB and PARN (Supplementary Figure S3). When lysate of HeLa cells expressing 5 × Flag-CPEB and 5 × Myc-PARN was immunoprecipitated with anti-Flag antibody, the precipitated fraction contained 5 × Myc-PARN. However, overexpression of a PARN mutant (PARN D28A) that had no deadenylase activity[29] showed no effect on CPEB-accelerated deadenylation and decay of the c-myc 3′-UTR reporter mRNA (data not shown). Collectively, these results indicate that CPEB-accelerated deadenylation and decay of the c-myc 3′-UTR reporter mRNA is dependent on the deadenylase activity of Caf1.

To confirm that Tob is involved in the CPEB-accelerated c-myc mRNA decay, small interfering RNA (siRNA)-mediated knockdown was performed. In this case, Tob and Tob2, a highly homologous paralogue of Tob, were depleted simultaneously (Figure 3f). As shown in Figures 3c and d, depletion of Tob/Tob2 significantly reduced the rate of mRNA decay of the c-myc 3′-UTR reporter.

Tob and CPEB negatively regulate endogenous c-myc expression at the mRNA level

We next examined if Tob as well as CPEB is actually involved in the regulation of endogenous c-myc mRNA. For this purpose, we used U2OS cells, as CPEB, Tob and Caf1. Proteins were all expressed in this cell line at a level sufficient for detection using our antibodies (Figure 4a). CPEB and Tob were depleted by siRNA-mediated knockdown, and the expression of c-myc was examined at both the mRNA and protein level. Depletion of Tob/Tob2 resulted in an

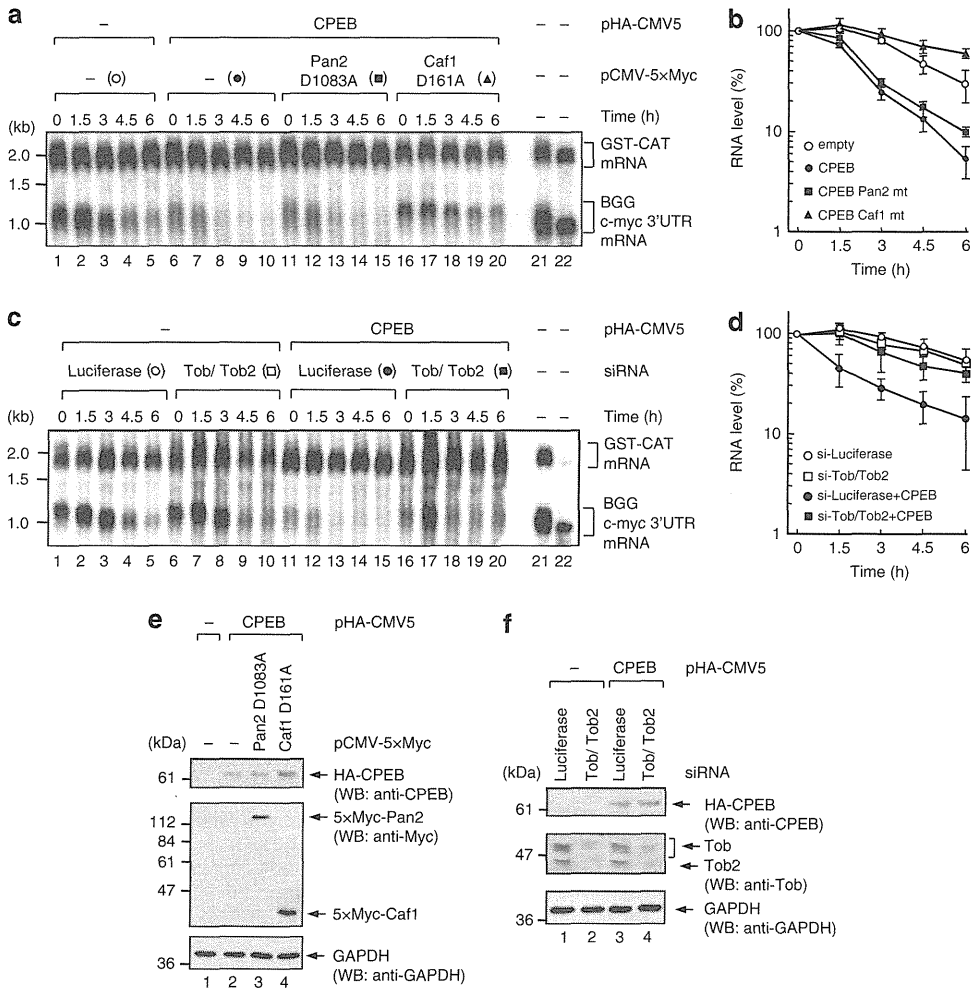

Figure 3. Tob–Caf1 complex is required for CPEB-mediated mRNA decay. (**a**) T-REx HeLa cells were transfected with the pFlag-CMV5/TO-BGG c-myc 3′-UTR reporter plasmid, pCMV-5 × Flag-GST-CAT reference plasmid, pHA-CMV5-CPEB (lanes 6–20), and either pCMV-5 × Myc-Pan2 D1083A (lanes 11–15) or pCMV-5 × Myc-Caf1 D161A (lanes 16–20). As a control, cells were transfected with pHA-CMV5 and pCMV-5 × Myc (lanes 1–5). After 1 day, BGG mRNA was induced to express by treatment with tetracycline for 2 h, and cells were harvested at the specified time after the transcription was shut off. BGG mRNA was induced to express by treatment with tetracycline for 12 h (steady state, lane 21), and digested with *RNase*H in the presence of oligo (dT) to mark the deadenylated mRNAs (lane 22). (**b**) The level of BGG c-myc 3′-UTR mRNA as in (**a**) was quantified and normalized by the level of GST-CAT mRNA. The score from the 0 h time point was defined as 100%. Data are the mean ± s.d. ($n = 3$). (**c**) HeLa cells were transfected with Tob/Tob2 or a control luciferase siRNA. At 48 h after siRNA transfection, cells were transfected with pFlag-CMV5/TO-BGG c-myc 3′-UTR reporter plasmid, pCMV-5 × Flag-GST-CAT reference plasmid, pcDNA-T7-TetR, and either pHA-CMV5-CPEB (lanes 11–20) or pHA-CMV5 (lanes 1–10). The transcriptional pulse-chase analysis was performed as described above. (**d**) The level of BGG c-myc 3′-UTR mRNA as in (**c**) was quantified and normalized by the level of GST-CAT mRNA. The score from the 0 h time point was defined as 100%. Data are the mean ± s.d. ($n = 3$). (**e**, **f**) Total cell lysate was analyzed by western blotting (WB) using indicated antibodies.

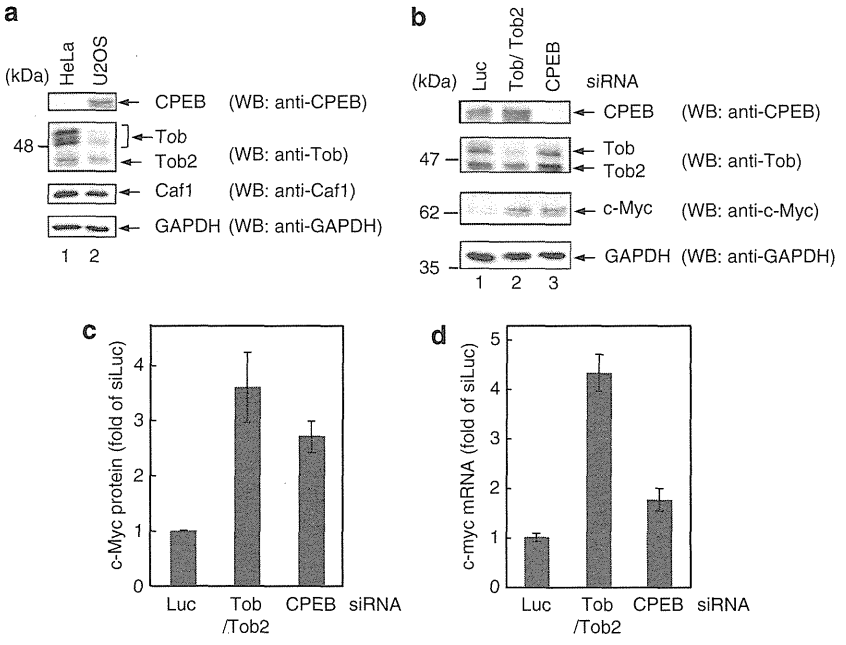

Figure 4. Downregulation of CPEB or Tob/Tob2 increases the levels of endogenous c-myc mRNA and protein in U2OS cells. (**a**) Whole cell lysate from U2OS or HeLa cells was analyzed by western blotting (WB) using the indicated antibodies. (**b**) U2OS cells were transfected with Tob/Tob2 siRNA, CPEB siRNA or a control luciferase siRNA. At 72 h after transfection, cells were harvested and total cell lysate was analyzed by WB using indicated antibodies. (**c**) The amount of c-Myc protein as in (**b**) was measured and normalized by GAPDH. The c-Myc protein level in luciferase siRNA-treated cells was set to 1 and fold-increases are indicated. Data are the mean ± s.d. ($n = 3$). (**d**) U2OS cells were transfected with Tob/Tob2 siRNA, CPEB siRNA or a control luciferase siRNA. At 72 h after transfection, total RNA was isolated and reverse-transcribed using random primer, and endogenous c-myc and GAPDH mRNA levels were analyzed by real-time PCR. The c-myc mRNA levels were normalized by GAPDH mRNA, and fold-increases are indicated with the c-myc mRNA level in luciferase siRNA-treated cells set to 1. Data are the mean ± s.d. ($n = 3$).

approximately three- to fourfold increase in c-myc expression at both levels (Figures 4b–d). Similar results were obtained for CPEB. c-myc expression at both the protein and mRNA level was increased by the depletion of CPEB, although relatively modestly (two- to threefold) (Figures 4b–d). These results indicate that CPEB and Tob form a ternary complex (CPEB–Tob–Caf1) and negatively regulate c-myc mRNA in cells.

Tob/Tob2 and CPEB negatively regulate the stability of endogenous c-myc mRNA in starved cells and the effects are abrogated by serum stimulation

It is well established that the level of c-myc mRNA depends upon the cellular growth state. In serum-starved cells, c-myc mRNA is expressed at a very low level. When cells are stimulated by serum, the abundance of c-myc mRNA starts to rise, and peaked within 1 and 2 h, followed by a decline and a plateau at several fold the levels in starved cells.[30] The transcription level reaches a peak before that of the c-myc mRNA level. As both Tob and CPEB regulate cell cycle progression, we examined whether these factors are involved in the serum-induced immediate-early response of c-myc gene expression (Figures 5b and c). To measure changes in the level of c-myc transcription and mRNA abundance at the same time, we performed a real-time polymerase chain reaction (PCR) analysis using two pairs of PCR primers (Figure 5a) and reverse transcription (RT) products of total RNA prepared from U2OS cells as a template. The primer pair a–c amplifies c-myc mature mRNA (cytoplasmic mRNA), whereas primer pair b and c amplifies c-myc pre-mRNA (nuclear mRNA). The pre-mRNA level generally reflects transcription. It is important to note that even after 35 thermal cycles, no amplification was observed when mock RT products prepared without reverse transcriptase were used as a template, and that these primer pairs amplify only a single band (Supplementary Figure S4A and data not shown). As shown in SupplementaryFigure S4B, the c-myc transcription and mRNA abundance measured in this assay system faithfully recapitulated the fluctuations previously reported upon serum stimulation, further validating the specificity of the primer pairs. Similar to the results from the steady-state analysis in Figure 4, knockdown of either Tob/Tob2 or CPEB resulted in a marked increase in c-myc mature mRNA in starved cells (Figure 5b, mature mRNA, starved, $P < 0.05$). However, the effect was attenuated at 1 h after serum stimulation (Figure 5b; mature mRNA, stimulated), suggesting that Tob/Tob2 and CPEB negatively regulate the level of c-myc mRNA under starved conditions and the effects are abrogated by serum stimulation. Analysis of pre-mRNA revealed that knockdown of Tob/Tob2 but not CPEB increased c-myc transcription slightly but significantly in starved condition (Figure 5b; pre-mRNA, $P < 0.05$). This result explains why c-myc mRNA was more abundant in Tob/Tob2 knockdown cells than in CPEB knockdown cells (Figure 4d). Figure 5c shows the same result as in Figure 5b, but the *y* axis represents the fold-increase of c-myc mature or pre-mRNA in serum-stimulated cells relative to starved cells. In control siRNA-treated cells, c-myc mature mRNA was increased by ~7-fold (Figure 5c, Luc, 2nd column). Knockdown of either Tob/Tob2 or CPEB reduced c-myc mRNA induction by ~3-fold after serum stimulation (Figure 5c; Tob/Tob2, CPEB, 2nd column, $P < 0.005$). In contrast, there were no significant differences in the induction of c-myc pre-mRNA among these cells (Figure 5c; Tob/Tob2, CPEB, 4th column). Consistent with fluctuations of c-myc mRNA, c-Myc protein was increased by knockdown of either Tob or CPEB in starved cells (Figures 5d and e). Also, serum-stimulated induction of c-Myc protein was inhibited by their knockdowns (Figures 5d and f). These results strengthen our conclusion that CPEB and Tob regulate the expression of c-Myc at the level of mRNA.

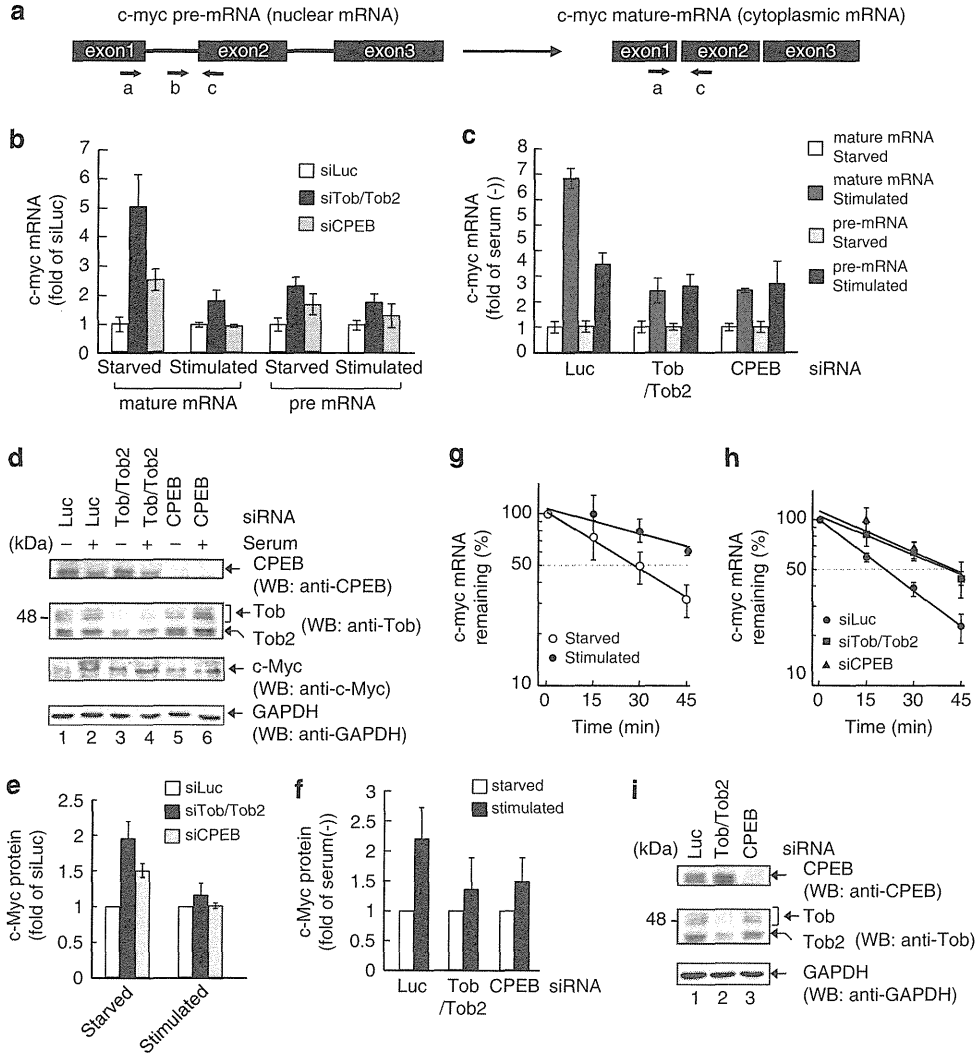

Figure 5. Tob/Tob2 and CPEB negatively regulate the stability of endogenous c-myc mRNA under starved conditions and the effects are abrogated by serum stimulation. (**a**) Diagram of c-myc mRNA and primers used for real-time PCR. Sense primers a and b correspond to sites within exon 1 and intron 1, respectively. Antisense primer c corresponds to exon 2. In this study, c-myc pre- and mature mRNA were amplified with primer pairs b–c and a–c, respectively. (**b**) U2OS cells were transfected with Tob/Tob2 siRNA, CPEB siRNA or a control luciferase siRNA. At 48 h after transfection, cells were washed and serum-starved for 24 h. Quiescent cells were stimulated with 10% fetal bovine serum (FBS) for 1 h, and total RNA was isolated and reverse-transcribed using random primer. Endogenous c-myc pre- and mature mRNA levels were analyzed by real-time PCR. The c-myc mRNA levels were normalized by GAPDH mRNA, and fold-increases are indicated with the c-myc mRNA level in luciferase siRNA-treated cells set to 1. Data are the mean ± s.d. ($n = 3$). (**c**) Data in (**b**) were analyzed and expressed with serum-starved samples set to 1. (**d**) U2OS cells were transfected with Tob/Tob2 siRNA, CPEB siRNA or a control luciferase siRNA. Total cell lysates were analyzed by western blotting (WB) using indicated antibodies. (**e**) The amount of c-Myc protein as in (**d**) was measured and normalized by GAPDH. The score in luciferase siRNA-treated cells was set to 1 and fold-increases are indicated. Data are the mean ± s.d. ($n = 3$). (**f**) Data in (**d**) were analyzed and expressed with serum-starved samples set to 1. (**g**) U2OS cells were washed and serum-starved for 24 h. Quiescent cells were pre-treated with 10 μg/ml actinomycin D for 15 min, and stimulated with 10% FBS or left untreated. Total RNA was isolated at the indicated times and reverse-transcribed using random primer. Endogenous c-myc mRNA levels (normalized by GAPDH mRNA) were analyzed by real-time PCR. The c-myc mRNA half-lives were 27.6 and 62.2 min in starved and stimulated cells, respectively. Data are the mean ± s.d. ($n = 3$). (**h**) U2OS cells were transfected with Tob/Tob2 siRNA, CPEB siRNA or a control luciferase siRNA. At 48 h after transfection, cells were washed and serum-starved for 24 h. Quiescent U2OS cells were treated with 10 μg/ml actinomycin D and 10% FBS. Total RNA was isolated and c-myc mRNA levels (normalized by GAPDH mRNA) were analyzed. The c-myc mRNA half-lives were 21.2, 38.8 and 37.0 min in control, Tob/Tob2 and CPEB knockdown cells, respectively. Data are the mean ± s.d. ($n = 3$). (**i**) Total cell lysate was analyzed by WB using indicated antibodies.

The above results led us to speculate that both Tob/Tob2 and CPEB are involved in the induction of c-myc mRNA expression after serum stimulation in a process of controlling mRNA stability. To investigate this possibility, we first examined if there are changes in c-myc mRNA stability after serum stimulation. Serum-starved U2OS cells were pre-treated with actinomycin D for 15 min, and then stimulated with serum or left untreated (starved). Actinomycin D was maintained in the medium throughout the time course. Total RNA was isolated every 15 min after serum was added and analyzed by real-time PCR. As shown in Figure 5g, the half-life of c-myc mRNA was about 2.3-fold longer in stimulated cells than starved cells. Thus, we next estimated the half-life of c-myc mRNA in serum-starved quiescent cells that were treated with siRNA against either Tob/Tob2 or CPEB (Figures 5h and i).

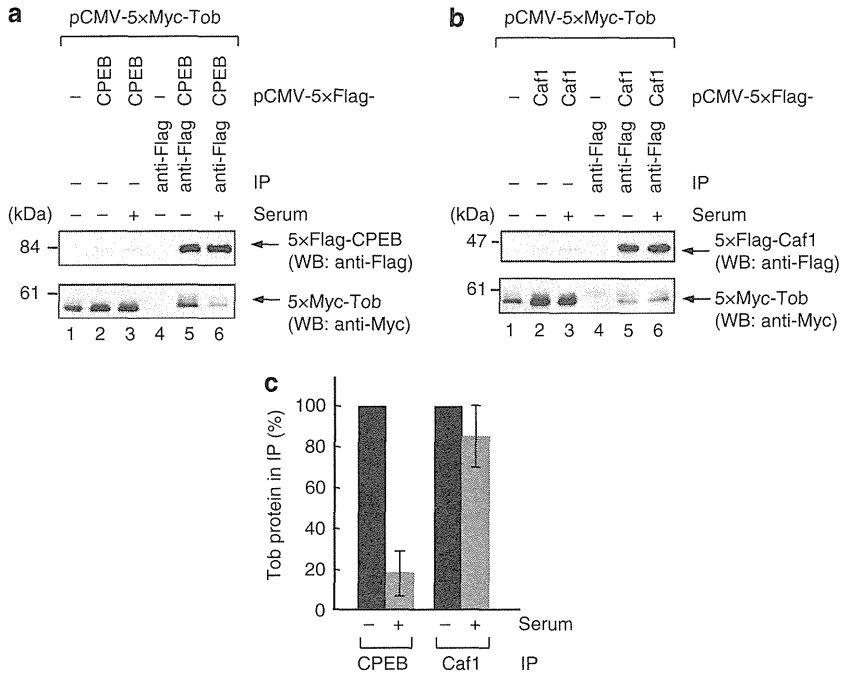

Figure 6. Serum stimulation induces dissociation of Tob and Caf1 from CPEB. (**a**) U2OS cells were transfected with pCMV-5 × Myc-Tob, and either pCMV-5 × Flag-CPEB or pCMV-5 × Flag. After 1 day, cells were washed and serum-starved for 24 h. The quiescent cells were stimulated with 10% fetal bovine serum (FBS) for 20 min and cell extracts were subjected to immunoprecipitation (IP) in the presence of *RNaseI* using anti-Flag antibody. The immunoprecipitates (lanes 4–6) and inputs (lanes 1–3) were analyzed by western blotting with the indicated antibodies. (**b**) U2OS cells were transfected with pCMV-5 × Myc-Tob, and either pCMV-5 × Flag-Caf1 or pCMV-5 × Flag. After 1 day, cells were washed and serum-starved for 24 h. The quiescent cells were stimulated with 10% serum for 20 min and cell extracts were subjected to IP in the presence of *RNaseI* using anti-Myc antibody. The immunoprecipitates (lanes 4–6) and inputs (lanes 1–3) were analyzed by western blotting with the indicated antibodies. (**c**) The amounts of the co-purified Tob proteins in the immunoprecipitates as in (**a**) and (**b**) were quantified and normalized by the amount of CPEB or Caf1 proteins immunoprecipitated. The score from serum-starved cells was defined as 100%. Data are the mean ± s.d ($n = 3$).

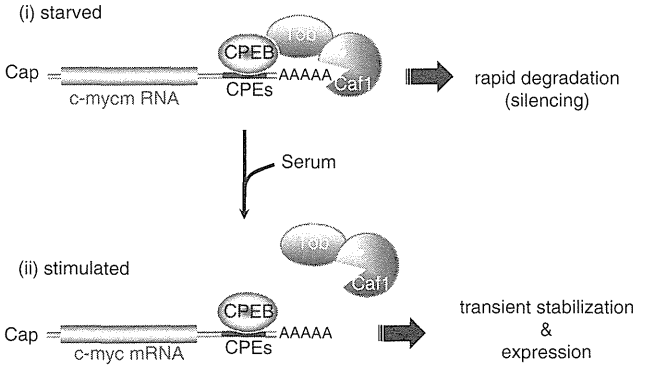

Figure 7. *Proposed model for the serum-induced stabilization of* c-myc mRNA. In serum-starved quiescent cells, CPEB bound to the *cis* elements (CPEs) in the c-myc mRNA 3′-UTR recruits the Tob–Caf1 complex to the mRNA to form a ternary complex, which leads to accelerated deadenylation and decay of the message. Upon serum stimulation, Tob and Caf1 transiently dissociate from CPEB and c-myc mRNA is stabilized and expressed as an 'immediate-early response gene'.

The half-life was extended in both Tob/Tob2 and CPEB knockdown cells by about twofold, near comparable to that in stimulated cells (2.3-fold as described above).

Tob and Caf1 dissociate from CPEB in response to serum stimulation

Finally, we performed co-immunoprecipitation experiments in serum-starved and -stimulated cells. When lysate of serum-starved U2OS cells expressing 5 × Flag-CPEB and 5 × Myc-Tob was immunoprecipitated with anti-Flag antibody, the precipitated fraction contained 5 × Myc-Tob as well as 5 × Flag-CPEB, whereas association of 5 × Myc-Tob with 5 × Flag-CPEB was drastically decreased after serum stimulation (Figures 6a and c, lanes 4–6, $P < 0.005$). In contrast, when lysate of serum-starved U2OS cells expressing 5 × Flag-Caf1 and 5 × Myc-Tob was immunoprecipitated with anti-Flag antibody, 5 × Myc-Tob was co-precipitated with 5 × Flag-Caf1 irrespective of the presence or absence of the serum, indicating that the binding of Tob with Caf1 was not affected by the serum condition (Figures 6b and c, lanes 4–6).

Taken together, our observations demonstrate that CPEB accelerates deadenylation and decay of the c-myc mRNA by recruiting the Tob–Caf1 complex to c-myc mRNA in starved quiescent cells, and serum stimulation induces dissociation of the Tob–Caf1 complex from CPEB to stabilize c-myc mRNA.

DISCUSSION

Tob is a member of the BTG/Tob family of antiproliferative proteins, which regulates cell cycle progression in a variety of cell types. Previous study demonstrated that Tob is involved in the control of G1- to S-phase transition of the cell cycle.[22,23] On the other hand, we and others have demonstrated that Tob functions in deadenylation of both general[16,17] and specific[19] mRNAs. However, the role of Tob in mRNA deadenylation with respect to cell growth regulation has remained to be determined.

This study provides evidence that Tob mediates deadenylation of c-myc mRNA and negatively regulates its expression. In serum-starved quiescent state, Tob mediates recruitment of Caf1 deadenylase to the CPEB-bound c-myc mRNA and accelerates deadenylation and decay of the mRNA. While in cells stimulated

by serum, Tob in a complex with Caf1 dissociates from CPEB-bound c-myc mRNA, which leads to a transient stabilization of the message and immediate-early expression of c-Myc (Figure 7). Thus, Tob appears to function in the control of cell growth at least, in part, by regulating the expression of c-myc.

It has been reported that CPEB activates translation of CPE-containing mRNAs (for example, αCAMKII and p53) by promoting cytoplasmic polyadenylation of the messages.[31,32] In contrast, no CPE-containing mRNA that is subject to accelerated deadenylation by CPEB has been reported in mammalian somatic cells. To our knowledge, c-myc is the first example of such an mRNA. Therefore, it was surprising that tethering CPEB to mRNA 3′-UTR led to accelerated deadenylation and decay of the mRNA (Supplementary Figure S2), which is reminiscent of c-myc, but neither αCAMK2 nor p53. Moreover, reporter mRNAs appended with other CPEB-target 3′-UTR, such as c-jun 3′-UTR,[33] were not affected by overexpression of CPEB (data not shown). Thus, CPEB does not necessarily induce polyadenylation (or deadenylation) of CPE-containing mRNAs by default. It remains unknown what determines whether CPEB-bound mRNAs will be degraded by accelerated deadenylation or translationally activated by cytoplasmic polyadenylation. In *Xenopus* oocytes, not every CPE-containing mRNA is translationally activated at the same time during meiosis after progesterone treatment. The positional distribution and the number of CPE sequences, as well as the arrangement of other *cis*-acting elements, such as AU-rich element,[34] Musashi-binding element,[35] Pumilio-binding element[36] and translational control sequence,[37] around CPEs define the extent and timing of translational activation.[38] Moreover, translational repression by CPEB requires a cluster of at least two CPEs with an optimal distance of 10–12 nucleotides.[36] This finding implies that the recruitment of the translational repressor maskin is mediated by a CPEB dimer formed on two adjacent CPEs. It is possible that such factors are involved in the determination of the fate of CPE-containing mRNAs in mammalian somatic cells. We are currently investigating this possibility.

c-Myc is a basic helix–loop–helix leucine zipper transcription factor and is required for the activation of cyclin D-dependent kinases and G0/G1- to S-phase transition.[39] Numerous studies have documented that the c-myc oncogene is expressed immediately after growth stimulation of quiescent cells and is essential for the regulation of cell growth. In most cases, changes measured in the rate of c-myc gene transcription are insufficient to account for the fluctuations and even no significant change in the rate of transcription was detectable in some cells.[30,40,41] These results suggest that the changes in c-myc expression during G0/G1- to S-phase transition are controlled by a post-transcriptional mechanism. However, this mechanism has remained to be determined for over 20 years. The results presented here provide one answer to this long-standing question.

Activation of c-myc gene expression after mitogenic stimulation is mediated by the Ras/Raf/mitogen-activated protein kinase pathway.[42] In this relation, previous study demonstrated that Tob is phosphorylated at serine residues by mitogen-activated protein kinase (Erk1/Erk2) downstream of the Ras signaling pathway.[22,23] These results led us to speculate that serum activates Ras-mitogen-activated protein kinase signaling pathways and the Erk-mediated phosphorylation of the serine residues of Tob is responsible for the dissociation of Tob from CPEB and stabilization of c-myc mRNA. However, mutant Tob with either serine-to-alanine or serine-to-glutamate mutations at the Erk phosphorylation sites (Ser 152, 154 and 164) bound CPEB with similar affinity to wild-type Tob and still showed dissociation from CPEB upon serum stimulation (data not shown). Previous study demonstrated that Tob is phosphorylated at at least three serine/threonine residues other than Ser 152, 154 and 164 upon mitogenic stimulation.[23] Thus, phosphorylation of residues other than the three serine residues or other modifications of Tob and/or CPEB seem to be responsible for the dissociation of the complex.

In addition to Tob and c-Myc, CPEB and Caf1 are also known to be involved in cell cycle regulation. (i) siRNA-mediated knockdown of CPEB results in an increase in astrocytic cell proliferation, whereas overexpression of CPEB inhibits it.[43] On the other hand, similar CPEB knockdown shows proliferation defects in HeLa cells.[44] (ii) siRNA-mediated knockdown of Caf1 leads to a defect in both G1- to S-phase transition and cell proliferation,[45] while overexpression of Caf1 also inhibits cell proliferation.[46] Thus, as in the case for Tob, Caf1 and CPEB also inhibit cell proliferation when overexpressed in cells, but the phenotypes resulting from siRNA-mediated knockdowns are divergent depending on cell types and on each component. Since CPEB also regulates cytoplasmic polyadenylation of cell cycle regulators (for example, CDKN3, Mnt, STXBP2, and so on) and Caf1 regulates transcription and deadenylation of general mRNAs, the effect on proliferation resulting from the modulation of these components might not be unidirectional.

Previous studies have shown that CPEB promotes polyadenylation-induced translational activation of cyclin B1 mRNA in the M phase and maskin-mediated translational repression in the S phase of early mitotic cell divisions in *Xenopus* embryos.[47] In contrast to the early embryonic divisions without intervening G1 and G2 phases, CPEB also regulates G2- to M-phase transition of mitotically dividing cells by mediating cytoplasmic polyadenylation of specific mRNAs, including CDKN3 and Cdc20.[44] In this study, we have shown that CPEB-mediated deadenylation and decay of c-myc mRNA might also be important for the regulation of G0/G1- to S-phase transition of the cell cycle. Remaining questions that we are currently pursuing are whether CPEB promotes cytoplasmic polyadenylation not only in the M phase but also during G0/G1- to S-phase transition and whether c-myc mRNA is polyadenylated in response to serum stimulation in a CPEB-dependent manner. These will be the subjects of forthcoming papers.

MATERIALS AND METHODS

Plasmids

To construct pHA-CMV5-CPEB, pCMV-5 × Myc-CPEB, pCMV-5 × Flag-CPEB, pMAL-cRI-CPEB and pGEX6P1-CPEB, the full-length open reading frame was PCR-amplified using the primers: sense, 5′-TTTCAATTGATG GCGTTCCCGCTGGAA-3′ and antisense, 5′-TTTGTCGACCTAGCTGGAA TCTCGGTTC-3′, and CPEB1 cDNA (IMAGE i.d. no. 6047179; Thermo Fischer Scientific, Waltham, MA, USA) as a template. The resulting DNA was digested with *Mun*I and *Sal*I and inserted into *Eco*RI and *Sal*I sites of pHA-CMV5, pCMV-5 × Myc, pCMV-5 × Flag, pMAL-cRI (New England Biolaboratories, Ipswich, MA, USA) and pGEX6P1 (GE Healthcare, Waukesha, WI, USA), respectively. To generate pCMV-5 × Myc-Tob, pME-Myc-Tob[19] was digested with *Eco*RI, and Tob cDNA fragment was inserted into the *Eco*RI site of pCMV-5 × Myc. To construct pCMV-5 × Myc-PARN, full-length PARN open reading frame was PCR-amplified using the primers: sense, 5′-A AGGTCGACATGGAGATAATCAGGAGC-3′ and antisense, 5′-AGAGTCGA CTTACCATGTGTCAGGAAC3′, and HeLa oligo(dT)-primed RT products. The resulting fragments were digested with *Sal*I and inserted into pCMV-5 × Myc. To construct pFlag-CMV5/TO-BGG c-myc 3′-UTR, pFlag-CMV5/TO-BGG(*Hind*III) was generated by introducing a *Hind*III site into the stop codon of pFlag-CMV5/TO-BGG using the primers: 5′-CTTGCTTTCTTG CTGTCCAATTTC-3′ and 5′-CTTAGTGATACTTGTGGGCCAGGG-3′. c-myc 3′-UTR was PCR-amplified using: sense, 5′-GAAAGCTTGTTCTAGAGG AAAAGTAAGGAA-3′ and antisense, 5′-GACGGTAGGATCCAGCTGGCTGCA GGTGAG-3′, and HeLa genomic DNA as a template. The resulting DNA was digested with *Hind*III and *Pst*I and inserted into pFlag-CMV5/TO-BGG(*Hind*III). To generate pFlag-CMV5/TO-BGG c-myc 3′-UTR CPE mt, the 3′, middle and 5′ segments of c-myc 3′-UTR were PCR-amplified using the following primer pairs: sense, 5′-GAAAGCTTGTTCTAGAGGAAAAGTAA GGAA-3′ and antisense, 5′-GTAAGCATCCAAAAGTTCTTTTATGCCCAA-3′; sense, 5′-AAGAACTTTTGGATGCTTACCATCTTTTTT-3′ and antisense, 5′-ACTT AAATCCAAAAAATTAGGGTTTATAGT-3′; and sense, 5′-CTAATTTTTTGGATT TAAGTACATTTTGCT-3′ and antisense, 5′-GACGGTAGGATCCAGCTGGC

TGCAGGTGAG-3′, respectively, and pFlag-CMV5/TO-BGG c-myc 3′-UTR as a template. The amplified fragments were mixed and used as a template for the second PCR conducted to generate full-length c-myc 3′-UTR fragment. The resulting fragment was digested with *Hind*III and *Pst*I and inserted into pFlag-CMV5/TO-BGG 3′-UTR(*Hind*III). The construction of pGEX6P1-Tob (1–285), pCMV-5 × Myc-Pan2 D1083A and pCMV-5 × Myc Caf1 D161A was described previously.[19]

siRNA

The sequences of siRNAs for luciferase, Tob and Tob2 were described previously.[19] CPEB siRNA consists of 5′-r (GACUCUGAAGAAACAGUUA) d(TT)-3′.

Antibodies

Antibodies used in this study were the following: anti-Flag (M2; Sigma, St Louis, MO, USA), anti-c-Myc (9E10 (Roche, Indianapolis, IN, USA); A-14, C-33 (Santa Cruz Technology, Santa Cruz, CA, USA)), anti-glyceraldehyde 3-phosphate dehydrogenase (GAPDH) (6C5; Millipore, Bedford, MA, USA), anti-GST (Z-5, Santa Cruz Technology), anti-MBP (New England Biolaboratories). Anti-Tob was raised against His-tagged Tob (1–110 amino acids). Anti-Caf1 (for immunoprecipitation), anti-CPEB and anti-PABPC1 were raised against His-tagged full-length proteins. Anti-Caf1 was a gift from Ann-Bin Shyu.[16]

Cell culture and transfection

HeLa, T-REx HeLa and U2OS cells were cultured in Dulbecco's modified Eagle's medium (Nissui, Tokyo, Japan) supplemented with 5% fetal bovine serum. U2OS cells were purchased from ATCC. DNA transfection was performed using Lipofectamine 2000 (Invitrogen, Carlsbad, CA, USA) as described previously.[17] For siRNA transfection, Lipofectamine RNAi MAX (Invitrogen) was used. For transfection with both siRNA and plasmid DNA, cells were first transfected with siRNA using RNAi MAX. After 24 h, cells were trypsinized, and re-cultured for another 24 h before DNA transfection using Lipofectamine 2000. Following further incubation for 24 h, pulse-chase experiments were conducted.

Immunoprecipitation

For immunoprecipitations, cells were lysed with 10 μg/ml RNaseA (Sigma) or 50 U/ml RNase I (New England Biolaboratories) in lysis buffer consisting of 50 mM Tris-HCl (pH 7.5), 50 mM NaCl, 0.25% Nonident P-40, 1 mM dithiothreitol, 2.5 mM ethylenediaminetetraacetic acid, 20 mM NaF, 10 mM $Na_4P_2O_7$, 0.1 mM phenylmethanesulfonylfluoride, 2 μg/ml aprotinin, and 2 μg/ml leupeptin. After centrifugation at 15 000 *g* for 20 min, the supernatant was incubated for 2 h at 4 °C with anti-Flag IgG agarose (Sigma), or anti-Myc agarose (Sigma). The resin was then washed three times with lysis buffer, and proteins retained on the resin were subjected to sodium dodecyl sulfate-polyacrylamide gel electrophoresis and western blot analysis.

GST-pull-down assay

GST-fused Tob and MBP-CPEB were produced in *E. coli* BL21 by adding 0.4 mM isopropylthio-β-galactoside and purified as described previously.[19] GST-fused Tob and MBP-CPEB were incubated with glutathione sepharose 4B (GE Healthcare) for 2 h at 4 °C in binding buffer (20 mM Tris-HCl (pH 7.5), 50 mM NaCl, 0.5% Nonident P-40, 1 mM dithiothreitol, 2.5 mM ethylenediaminetetraacetic acid). The resin was then washed three times with binding buffer. Bound proteins were eluted with sodium dodecyl sulfate-polyacrylamide gel electrophoresis sample buffer and analyzed by western blotting.

Northern blot analysis

The northern blot analysis, transcriptional pulse-chase analysis and oligo (dT)-RNase H treatment of mRNA to generate poly(A)$^-$ mRNA were performed as described previously,[19] except that the pulse transcription was induced by 10 ng/ml tetracycline for 2 h.

Real-time PCR analysis

Cells were directly harvested (steady-state level) or treated with 10 μg/ml actinomycin D (mRNA decay) and harvested at indicated times. Total RNA was isolated by the acid guanidinium–phenol–chloroform method with minor modifications and genomic DNA was removed by digestion with DNase I for 30 min. Random-primed RT of RNA (1.5 μg) was performed using SuperScript III Reverse Transcriptase (Invitrogen). Real-time PCR analysis was performed using StepOne Real-Time PCR system with PowerSYBR Green PCR Master Mix (Applied Biosystems, Foster City, CA, USA). Changes in c-myc mRNA levels were determined by the relative standard curve method using GAPDH mRNA for internal normalization. The primers for GAPDH were described previously.[19] c-myc mRNA was amplified using primers: sense, 5′-TTCGGGTAGTGGAAAACCAG-3′ and antisense, 5′-GGAACTATGACCTCGACTACGACT-3′. C-myc pre-mRNA was amplified using: sense, 5′-GCACCAAGACCCCTTTAACT-3′ and antisense, 5′-GGAAC;TATGACCTCGACTACGACT-3′. The specificity of the primer pairs and genomic DNA digestion were checked by PCR analysis using KOD FX (TOYOBO, Osaka, Japan) or PowerSYBR Green (Applied Biosystems).

CONFLICT OF INTEREST

The authors declare no conflict of interest.

ACKNOWLEDGEMENTS

We thank A-B Shyu for anti-Caf1 antibody. This work was supported by a Grant-in-Aid for Scientific Research on Innovative Areas 'RNA regulation' (No. 20112006) from the Ministry of Education, Culture, Sports, Science and Technology of Japan.

REFERENCES

1 Gallie DR. The cap and poly(A) tail function synergistically to regulate mRNA translational efficiency. *Genes Dev* 1991; **5**: 2108–2116.
2 Iizuka N, Najita L, Franzusoff A, Sarnow P. Cap-dependent and cap-independent translation by internal initiation of mRNAs in cell extracts prepared from *Saccharomyces cerevisiae*. *Mol Cell Biol* 1994; **14**: 7322–7330.
3 Decker CJ, Parker R. A turnover pathway for both stable and unstable mRNAs in yeast: evidence for a requirement for deadenylation. *Genes Dev* 1993; **7**: 1632–1643.
4 Wu X, Brewer G. The regulation of mRNA stability in mammalian cells: 2.0. *Gene* 2012; **500**: 10–21.
5 Eckmann CR, Rammelt C, Wahle E. Control of poly(A) tail length. *Wiley Interdiscip Rev RNA* 2011; **2**: 348–361.
6 Korner CG, Wormington M, Muckenthaler M, Schneider S, Dehlin E, Wahle E. The deadenylating nuclease (DAN) is involved in poly(A) tail removal during the meiotic maturation of *Xenopus* oocytes. *EMBO J* 1998; **17**: 5427–5437.
7 Barnard DC, Ryan K, Manley JL, Richter JD. Symplekin and xGLD-2 are required for CPEB-mediated cytoplasmic polyadenylation. *Cell* 2004; **119**: 641–651.
8 Kim JH, Richter JD. Opposing polymerase-deadenylase activities regulate cytoplasmic polyadenylation. *Mol Cell* 2006; **24**: 173–183.
9 Yamashita A, Chang TC, Yamashita Y, Zhu W, Zhong Z, Chen CY *et al.* Concerted action of poly(A) nucleases and decapping enzyme in mammalian mRNA turnover. *Nat Struct Mol Biol* 2005; **12**: 1054–1063.
10 Uchida N, Hoshino S, Katada T. Identification of a human cytoplasmic poly(A) nuclease complex stimulated by poly(A)-binding protein. *J Biol Chem* 2004; **279**: 1383–1391.
11 Bianchin C, Mauxion F, Sentis S, Seraphin B, Corbo L. Conservation of the deadenylase activity of proteins of the Caf1 family in human. *RNA* 2005; **11**: 487–494.
12 Chen J, Chiang YC, Denis CL. CCR4 a 3′–5′ poly(A) RNA and ssDNA exonuclease, is the catalytic component of the cytoplasmic deadenylase. *EMBO J* 2002; **21**: 1414–1426.
13 Viswanathan P, Ohn T, Chiang YC, Chen J, Denis CL. Mouse CAF1 can function as a processive deadenylase/3′–5′-exonuclease in vitro but in yeast the deadenylase function of CAF1 is not required for mRNA poly(A) removal. *J Biol Chem* 2004; **279**: 23988–23995.
14 Ikematsu N, Yoshida Y, Kawamura-Tsuzuku J, Ohsugi M, Onda M, Hirai M *et al.* Tob2, a novel anti-proliferative Tob/BTG1 family member, associates with a component of the CCR4 transcriptional regulatory complex capable of binding cyclin-dependent kinases. *Oncogene* 1999; **18**: 7432–7441.
15 Okochi K, Suzuki T, Inoue J, Matsuda S, Yamamoto T. Interaction of anti-proliferative protein Tob with poly(A)-binding protein and inducible poly(A)-binding protein: implication of Tob in translational control. *Genes Cells* 2005; **10**: 151–163.
16 Ezzeddine N, Chang TC, Zhu W, Yamashita A, Chen CY, Zhong Z *et al.* Human TOB, an antiproliferative transcription factor, is a poly(A)-binding protein-dependent positive regulator of cytoplasmic mRNA deadenylation. *Mol Cell Biol* 2007; **27**: 7791–7801.

17 Funakoshi Y, Doi Y, Hosoda N, Uchida N, Osawa M, Shimada I *et al.* Mechanism of mRNA deadenylation: evidence for a molecular interplay between translation termination factor eRF3 and mRNA deadenylases. *Genes Dev* 2007; **21**: 3135–3148.
18 Ruan L, Osawa M, Hosoda N, Imai S, Machiyama A, Katada T *et al.* Quantitative characterization of Tob interactions provides the thermodynamic basis for translation termination-coupled deadenylase regulation. *J Biol Chem* 2010; **285**: 27624–27631.
19 Hosoda N, Funakoshi Y, Hirasawa M, Yamagishi R, Asano Y, Miyagawa R *et al.* Anti-proliferative protein Tob negatively regulates CPEB3 target by recruiting Caf1 deadenylase. *EMBO J* 2011; **30**: 1311–1323.
20 Jin M, Wang XM, Tu Y, Zhang XH, Gao X, Guo N *et al.* The negative cell cycle regulator, Tob (transducer of ErbB-2), is a multifunctional protein involved in hippocampus-dependent learning and memory. *Neuroscience* 2005; **131**: 647–659.
21 Wang XM, Gao X, Zhang XH, Tu YY, Jin ML, Zhao GP *et al.* The negative cell cycle regulator, Tob (transducer of ErbB-2), is involved in motor skill learning. *Biochem Biophys Res Commun* 2006; **340**: 1023–1027.
22 Maekawa M, Nishida E, Tanoue T.. Identification of the Anti-proliferative protein Tob as a MAPK substrate. *J Biol Chem* 2002; **277**: 37783–37787.
23 Suzuki T, K-Tsuzuku J, Ajima R, Nakamura T, Yoshida Y, Yamamoto T. Phosphorylation of three regulatory serines of Tob by Erk1 and Erk2 is required for Ras-mediated cell proliferation and transformation. *Genes Dev* 2002; **16**: 1356–1370.
24 Ellis RE, Kimble J. The fog-3 gene and regulation of cell fate in the germ line of *Caenorhabditis elegans*. *Genetics* 1995; **139**: 561–577.
25 Xiong B, Rui Y, Zhang M, Shi K, Jia S, Tian T *et al.* Tob1 controls dorsal development of zebrafish embryos by antagonizing maternal beta-catenin transcriptional activity. *Dev Cell* 2006; **11**: 225–238.
26 Yoshida Y, Tanaka S, Umemori H, Minowa O, Usui M, Ikematsu N *et al.* Negative regulation of BMP/Smad signaling by Tob in osteoblasts. *Cell* 2000; **103**: 1085–1097.
27 Tzachanis D, Freeman GJ, Hirano N, van Puijenbroek AA, Delfs MW, Berezovskaya A *et al.* Tob is a negative regulator of activation that is expressed in anergic and quiescent T cells. *Nat Immunol* 2011; **2**: 1174–1182.
28 Groisman I, Ivshina M, Marin V, Kennedy NJ, Davis RJ, Richter JD. Control of cellular senescence by CPEB. *Genes Dev* 2006; **20**: 2701–2712.
29 Ren YG, Martinez J, Virtanen A. Identification of the active site of poly(A)-specific ribonuclease by site-directed mutagenesis and Fe(2+)-mediated cleavage. *J Biol Chem* 2002; **277**: 5982–5987.
30 Dean M, Levine RA, Ran W, Kindy MS, Sonenshein GE, Campisi J. Regulation of c-myc transcription and mRNA abundance by serum growth factors and cell contact. *J Biol Chem* 1986; **261**: 9161–9166.
31 Burns DM, Richter JD. CPEB regulation of human cellular senescence, energy metabolism, and p53 mRNA translation. *Genes Dev* 2008; **22**: 3449–3460.
32 Wu L, Wells D, Tay J, Mendis D, Abbott MA, Barnitt A *et al.* CPEB-mediated cytoplasmic polyadenylation and the regulation of experience-dependent translation of alpha-CaMKII mRNA at synapses. *Neuron* 1998; **21**: 1129–1139.
33 Zearfoss NR, Alarcon JM, Trifilieff P, Kandel E, Richter JD. A molecular circuit composed of CPEB-1 and c-Jun controls growth hormone-mediated synaptic plasticity in the mouse hippocampus. *J Neurosci* 2008; **28**: 8502–8509.
34 Belloc E, Mendez R. A deadenylation negative feedback mechanism governs meiotic metaphase arrest. *Nature* 2008; **452**: 1017–1021.
35 Arumugam K, Wang Y, Hardy LL, MacNicol MC, MacNicol AM. Enforcing temporal control of maternal mRNA translation during oocyte cell-cycle progression. *EMBO J* 2010; **29**: 387–97.
36 Pique M, Lopez JM, Foissac S, Guigo R, Mendez R. A combinatorial code for CPE-mediated translational control. *Cell* 2008; **132**: 434–448.
37 Wang YY, Charlesworth A, Byrd SM, Gregerson R, MacNicol MC, MacNicol AM. A novel mRNA 3′ untranslated region translational control sequence regulates *Xenopus* Wee1 mRNA translation. *Dev Biol* 2008; **317**: 454–466.
38 MacNicol MC, MacNicol AM. Developmental timing of mRNA translation—integration of distinct regulatory elements. *Mol Reprod Dev* 2010; **77**: 662–669.
39 Mateyak MK, Obaya AJ, Sedivy JM. c-Myc regulates cyclin D-Cdk4 and -Cdk6 activity but affects cell cycle progression at multiple independent points. *Mol Cell Biol* 1999; **19**: 4672–4683.
40 Blanchard JM, Piechaczyk M, Dani C, Chambard JC, Franchi A, Pouyssegur J *et al.* C-myc gene is transcribed at high rate in G0-arrested fibroblasts and is post-transcriptionally regulated in response to growth factors. *Nature* 1985; **317**: 443–445.
41 Kindy MS, Sonenshein GE. Regulation of oncogene expression in cultured aortic smooth muscle cells. Post-transcriptional control of c-myc mRNA. *J Biol Chem* 1986; **261**: 12865–12868.
42 Kerkhoff E, Houben R, Loffler S, Troppmair J, Lee JE, Rapp UR. Regulation of c-myc expression by Ras/Raf signalling. *Oncogene* 1998; **16**: 211–216.
43 Kim KC, Oh WJ, Ko KH, Shin CY, Wells DG. Cyclin B1 expression regulated by cytoplasmic polyadenylation element binding protein in astrocytes. *J Neurosci* 2011; **31**: 12118–12128.
44 Novoa I, Gallego J, Ferreira PG, Mendez R. Mitotic cell-cycle progression is regulated by CPEB1 and CPEB4-dependent translational control. *Nat Cell Biol* 2010; **12**: 447–456.
45 Aslam A, Mittal S, Koch F, Andrau JC, Winkler GS. The Ccr4-NOT deadenylase subunits CNOT7 and CNOT8 have overlapping roles and modulate cell proliferation. *Mol Biol Cell* 2009; **20**: 3840–3850.
46 Horiuchi M, Takeuchi K, Noda N, Muroya N, Suzuki T, Nakamura T *et al.* Structural basis for the antiproliferative activity of the Tob–hCaf1 complex. *J Biol Chem* 2009; **284**: 13244–13255.
47 Groisman I, Jung MY, Sarkissian M, Cao Q, Richter JD. Translational control of the embryonic cell cycle. *Cell* 2002; **109**: 473–483.

Supplementary Information accompanies the paper on the Oncogene website (http://www.nature.com/onc)

RNA
A PUBLICATION OF THE RNA SOCIETY

Biological role of the two overlapping poly(A)-binding protein interacting motifs 2 (PAM2) of eukaryotic releasing factor eRF3 in mRNA decay

Masanori Osawa, Nao Hosoda, Tamiji Nakanishi, et al.

RNA published online September 27, 2012
Access the most recent version at doi:10.1261/rna.035311.112

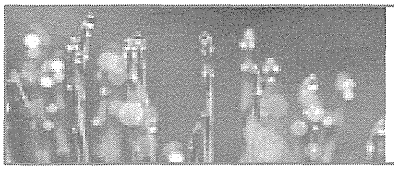

Biological role of the two overlapping poly(A)-binding protein interacting motifs 2 (PAM2) of eukaryotic releasing factor eRF3 in mRNA decay

MASANORI OSAWA,[1] NAO HOSODA,[2] TAMIJI NAKANISHI,[1] NAOYUKI UCHIDA,[3] TOMOMI KIMURA,[1] SHUNSUKE IMAI,[1] ASAKO MACHIYAMA,[1] TOSHIAKI KATADA,[3] SHIN-ICHI HOSHINO,[2] and ICHIO SHIMADA[1,4,5]

[1]Department of Physical Chemistry, Graduate School of Pharmaceutical Sciences, The University of Tokyo, Tokyo 113-0033, Japan
[2]Department of Biological Chemistry, Graduate School of Pharmaceutical Sciences, Nagoya City University, Nagoya 467-8603, Japan
[3]Department of Physiological Chemistry, Graduate School of Pharmaceutical Sciences, The University of Tokyo, Tokyo 113-0033, Japan
[4]Biomedicinal Information Research Center (BIRC), National Institute of Advanced Industrial Science and Technology (AIST), Tokyo 135-0064, Japan

ABSTRACT

Eukaryotic releasing factor GSPT/eRF3 mediates translation termination-coupled mRNA decay via interaction with a cytosolic poly(A)-binding protein (PABPC1). A region of eRF3 containing two overlapping PAM2 (PABPC1-interacting motif 2) motifs is assumed to bind to the PABC domain of PABPC1, on the poly(A) tail of mRNA. PAM2 motifs are also found in the major deadenylases Caf1–Ccr4 and Pan2–Pan3, whose activities are enhanced upon PABPC1 binding to these motifs. Their deadenylase activities are regulated by eRF3, in which two overlapping PAM2 motifs competitively prevent interaction with PABPC1. However, it is unclear how these overlapping motifs recognize PABC and regulate deadenylase activity in a translation termination-coupled manner. We used a dominant-negative approach to demonstrate that the N-terminal PAM2 motif is critical for eRF3 binding to PABPC1 and that both motifs are required for function. Isothermal titration calorimetry (ITC) and NMR analyses revealed that the interaction is in equilibrium between the two PAM2–PABC complexes, where only one of the two overlapping PAM2 motifs is PABC-bound and the other is PABC-unbound and partially accessible to the other PABC. Based on these results, we proposed a biological role for the overlapping PAM2 motifs in the regulation of deadenylase accessibility to PABPC1 at the 3′ end of poly(A).

Keywords: translation; mRNA decay; eRF3; poly(A)-binding protein; PAM2; chemical exchange

INTRODUCTION

Degradation of mRNA (mRNA decay) is an important process for the down-regulation of gene expression. General decay of eukaryotic mRNA occurs via shortening of the 3′-poly(A) tail (deadenylation), which is a rate-limiting step for mRNA decay (Decker and Parker 1993; Fritz et al. 2004; Meyer et al. 2004; Parker and Song 2004).

Deadenylation is mediated by two cytoplasmic deadenylase complexes, Pan2–Pan3 and Caf1–Ccr4 (Daugeron et al. 2001; Tucker et al. 2001; Yamashita et al. 2005). Pan2 and Pan3 are catalytic and regulatory subunits, respectively (Sachs and Deardorff 1992; Uchida et al. 2004), while Caf1 and Ccr4 possess deadenylase activity (Tucker et al. 2001; Chen et al. 2002; Bianchin et al. 2005). Caf1 interacts with anti-proliferative proteins Tob (Tob1) and Tob2, members of the BTG/Tob family (Ikematsu et al. 1999; Prevot et al. 2001; Yoshida et al. 2001) unique to metazoa (Tirone 2001; Jia and Meng 2007). Tob/Tob2 consists of an N-terminal BTG domain responsible for Caf1 binding (Mauxion et al. 2009) and a C-terminal unstructured region (Ruan et al. 2010).

In mammalian cells, the catalytic activities of these deadenylase complexes are enhanced by poly(A)-binding protein (PABPC1), which tightly associates with the 3′-poly(A) tail (Uchida et al. 2004; Ezzeddine et al. 2007; Funakoshi et al. 2007). Interaction with PABPC1 recruits the deadenylase complexes to their substrate, the 3′-poly(A) tail, enhancing catalytic activity. Mutagenesis studies identified the direct binding sites as the C-terminal domain of PABPC1, referred to as PABC (residues 541–623 in human PABPC1), and PABPC1-binding motif 2 (PAM2) in Pan3 and Tob (Fig. 1; Ezzeddine et al. 2007; Funakoshi et al. 2007; Siddiqui et al. 2007).

[5]**Corresponding author**
E-mail shimada@iw-nmr.f.u-tokyo.ac.jp
Article published online ahead of print. Article and publication date are at http://www.rnajournal.org/cgi/doi/10.1261/rna.035311.112.

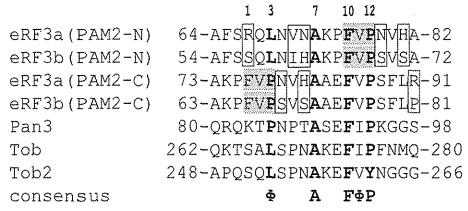

FIGURE 1. Sequence alignment of the PAM2 motifs. Numbers *above* the sequences indicate positions in the PAM2 motif (Kozlov et al. 2004). Numbers at both ends of the sequences represent residue numbers in mouse eRF3a/b, human Pan3 (Uchida et al. 2004), Tob (Ruan et al. 2010), and Tob2 (Kozlov et al. 2004). The unconserved residues between eRF3a and b are enclosed by rectangles. (Green) The overlapped residues of eRF3 within 12 residues of PAM2.

We demonstrated that deadenylation is mediated by a complex of eukaryotic releasing factors eRF3 and eRF1, coupled to translation termination (Funakoshi et al. 2007). eRF1 recognizes all three stop codons, releasing newly synthesized polypeptides from ribosomes (Frolova et al. 1994). eRF3 contains a conserved GTPase domain that binds to the C terminus of eRF1, which mediates GTP-dependent translation termination (Zhouravleva et al. 1995). The N terminus of eRF3, which is less conserved among eukaryotes, associates with the C terminus of PABPC1 (Hoshino et al. 1999b), in which the direct binding sites are PABC in PABPC1 and PAM2 in eRF3 (Fig. 1; Funakoshi et al. 2007). It should be noted that there is no PAM2 in yeast eRF3 (Kononenko et al. 2010), and PABC in yeast Pab1p is less well conserved from mammalian PABPC1 (Kozlov et al. 2002). Therefore, the interaction mode between Pab1p and eRF3 in yeast differs from that in mammals, although the interaction is evolutionarily conserved (Hoshino et al. 1999a; Kozlov et al. 2001; Cosson et al. 2002; Uchida et al. 2002; Hosoda et al. 2003). PAM2 was reported as the second PABPC1 binding motif in Paip2 (Roy et al. 2002), which is found in several metazoan proteins (Albrecht and Lengauer 2004). The consensus sequence is "xxΦxxxAxxFΦP" (x: any amino acid, Φ: hydrophobic amino acid) (Albrecht and Lengauer 2004), in which the well-conserved phenylalanine residue at position 10 is critical to PABC binding affinity (Kozlov et al. 2004; Kozlov and Gehring 2010; Kozlov et al. 2010). Indeed, alanine substitution of the phenylalanine residue of PAM2 in Paip2 diminished its binding affinity (Kozlov et al. 2004).

In our previous report (Funakoshi et al. 2007), we demonstrated that translation termination-coupled deadenylation was slowed by mutation of the region containing the well-conserved tenth Phe residue of PAM2 motif(s) in eRF3, Pan3, or Tob. Furthermore, interaction of the deadenylases with PABPC1 is competitively inhibited by eRF3. Based on these results, we proposed a working model of deadenylation: The termination complex, eRF1–eRF3, which dominantly associates with PABC in poly(A)-bound PABPC1, is recruited from the PABC domain to the ribosomes upon translational termination, increasing the catalytic activities of the deadenylase complexes by allowing them to access PABC on poly(A)-bound PABPC1 and the 3′ end of poly(A) (Funakoshi et al. 2007). Therefore, competitive interaction of eRF1–eRF3, Pan2–Pan3, and Caf1–Ccr4 with PABC plays a central role in coupling translation termination and deadenylation.

Interestingly, eRF3 possesses two PAM2 motifs (residues 67–78 and 76–87 in eRF3a, referred to as PAM2-N and PAM2-C, respectively) that partially overlap (Fig. 1). Among a variety of PAM2-containing proteins, the overlapping PAM2 motifs are only found in eRF3 and are distributed widely in metazoan eRF3s (Kononenko et al. 2010). Although the PAM2-C motif—but not PAM2-N—in eRF3 reportedly plays a critical role in PABPC1 binding (Kononenko et al. 2010), a previous study indicated that either PAM2 motif peptide is active for PABC binding (Kozlov et al. 2004). The crystal structures of PABC in complex with peptides containing PAM2-N or PAM2-C have been reported (Kozlov and Gehring 2010). Therefore, the overlapping PAM2 motifs seem to provide eRF3 with a notable function among the many PAM2-containing proteins. However, the physiological function of these eRF3 motifs in translation termination-dependent regulation of deadenylase activity has remained elusive.

Here, we demonstrated that dominant-negative mutants of either PAM2 motif slowed eRF3-mediated deadenylation, showing that both are required for function. Isothermal titration calorimetry (ITC) and NMR analyses revealed that the interaction is in equilibrium between the two states, where either PAM2-N or PAM2-C of eRF3 binds to PABC of PABPC1. These results indicate that when one of the PAM2 motifs of eRF3 binds to PABC, another PAM2 is partially accessible to the other PABC. Based on these results, we propose a biological role for the PAM2 motifs in the regulation of deadenylase accessibility to the PABPC1 molecule at the 3′ end of poly(A).

RESULTS

Both PAM2 motifs mediate poly(A) degradation

To explore the roles of the overlapping PAM2 motifs in eRF3, we prepared single alanine mutants of the phenylalanine residues at position 10 of the PAM2-N and C motifs (F66A and F75A of eRF3b); each is supposed to inactivate a single motif, which left the other active. In addition, we prepared a double mutant (F66A/F75A) to abolish affinity for PABPC1 (see below for the effects of these mutations on PABC binding affinity). The effect of ectopic expression of these mutants and wild-type eRF3b on eRF3-mediated mRNA normal decay was assessed by a dominant-negative approach.

First, HeLa cells were cotransfected with a β-globin reporter plasmid, a plasmid expressing tetracycline repressor, a reference plasmid expressing 5xFlag-EGFP as a transfection/

loading control, and a plasmid expressing either 5xMyc-eRF3b or a mutant derivative (F66A, F75A, or F66A/F75A). Deadenylation kinetics were examined by transcriptional pulse-chase experiments (Fig. 2A,B). Transcription of the reporter gene was driven by pulsed addition of tetracycline and metabolism of the newly transcribed mRNAs was followed after transcription shut-off by removal of tetracycline from the culture medium. Overexpression of F66A, F75A, or F66A/F75A to ~10-fold the level of endogenous eRF3 (Supplemental Fig. 1) suppressed the rate of deadenylation and significantly prolonged mRNA half-life. The mutants had no effect on translation termination in a translational read-through assay (Supplemental Fig. 2).

Then, we examined dominant-negative binding of these mutants to cellular PABPC1. Figure 2C (lanes 1–5) indicates that comparable levels of eRF3b protein were expressed, as shown in Supplemental Figure 1. Coimmunoprecipitation (Fig. 2C, lanes 6–8) indicated that the overexpressed eRF3 and F75A mutant competitively excluded endogenous eRF3 from cellular PABPC1, while the F66A and F66A/F75A mutants did not. These results strongly suggest that PAM2-N—which is active in the F75A mutant and inactive in the F66A and F66A/F75A mutants—is critical for binding to PABPC1, while PAM2-C, which is inactivated by the F75A mutant, mediates acceleration of deadenylation, thereby shortening of the mRNA half-life.

The PABC binding site on eRF3a is located within residues 64–94

To physicochemically characterize the interaction between eRF3 and PABPC1, we first aimed to identify the PABC binding site on eRF3 by ITC and NMR analyses. Here, we used fragments of eRF3a, instead of eRF3b, because the amount of the bacterial expression of the eRF3a fragments was larger than that of eRF3b. Since the PAM2 sequences lie between residues 67 and 87 in eRF3a (residues 67–78 and 76–87 for PAM2-N and PAM2-C, respectively), we compared the PABC binding affinity of the entire N-terminal region of eRF3a (residues 1–207) with those of the truncated eRF3a fragments, residues 51–102 and residues 64–94, both of which contain the overlapping PAM2 sequences, to see whether any other region contributes to PABC binding.

Fitting of the ITC results (Fig. 3; Table 1) provided comparable dissociation constants (K_d) of 0.4–2.3 μM with a binding stoichiometry of 1:1 for the three regions of eRF3a tested, indicating that the PABC binding site lies within residues 64–94 of eRF3a. Slightly higher affinity for the shorter fragment suggests that the shorter peptide possesses more flexibility to fit the binding site on PABC.

Then, we observed the ^{1}H–^{15}N HSQC spectra of ^{15}N-labeled eRF3a (residues 51–102) in the presence or absence of PABC. The spectrum in the PABC-free state exhibited narrow signal dispersion in the ^{1}H dimension, indicating that this region is unstructured (Fig. 4A, black). Upon addition of PABC to ^{15}N-labeled eRF3a(51–102), chemical shift changes and significant line broadening were observed (Fig. 4A, red). Broadening was also reported for the interaction of eRF3a (residues 64–91) with PABC (Kozlov et al. 2004). Backbone assignments obtained by a series of triple resonance experiments using uniformly ^{13}C,^{15}N-labeled eRF3a(51–102) revealed that the signals perturbed by the addition of PABC were for residues 64–94.

We concluded that the PABC-binding site on eRF3a is located within residues 64–94.

Only one PAM2 motif at a time interacts with PABC

Further ITC analyses were performed to characterize PABC binding of eRF3a(64–94) single mutants [position 10 in PAM2-N (F76A) and PAM2-C (F85A)] and the double mutant F76A/F85A, each of which corresponds to F66A, F75A, and F66A/F75A of eRF3b in Figure 2 (see also Fig. 1). K_d values of 11 and 0.8 μM with a binding stoichiometry of 1:1 were obtained for the F76A and F85A mutants, respectively. These results indicate that PAM2-N possesses higher affinity for PABC than PAM2-C, which is consistent with the results of the coimmunoprecipitation analysis (Fig. 2C). The double mutant F66A/F75A showed no heat exchange reflecting binding (Table 1).

In addition, ITC analyses for several shorter eRF3a fragments (Fig. 3B) revealed that eRF3a residues 64–82 and 73–94, containing PAM2-N and PAM2-C, respectively, exhibited K_d values of 0.82 and 2.9 μM and a binding stoichiometry of 1:1. These values are comparable to those obtained with fragments containing both PAM2 motifs (residues 1–207, 51–102, and 64–94) (Table 1). On the other hand, fragments containing an incomplete PAM2 motif (peptides derived from residues 64–75, 64–78, 76–94, and 79–94) exhibited impaired affinity. These results indicate that the PABC interaction can occur at either PAM2 motif.

We prepared a synthetic peptide containing the two PAM2 motifs of eRF3 separated by a 6-residue repeat (residues 64–81 followed by 76–94) (Fig. 3B). Although a similar K_d of 3.1 μM was obtained for the interaction between this peptide and PABC, the binding stoichiometry was 1:2 (Table 1), supporting the notion that simultaneous binding of two PABC molecules to an eRF3a molecule is precluded by the overlap of the two PAM2 motifs, despite both motifs being able to bind PABC.

We concluded that both PAM2 motifs in eRF3 can bind to PABC, although PAM2-N possesses higher affinity than PAM2-C, and either motif can bind to PABC at a time.

Binding of eRF3 to PABC with chemical exchange between the two complexes: PABC in complex with PAM2-N and PAM2-C

We investigated the spectral changes of ^{15}N-labeled PABC upon interaction with eRF3a(64–82) and eRF3a(73–94),

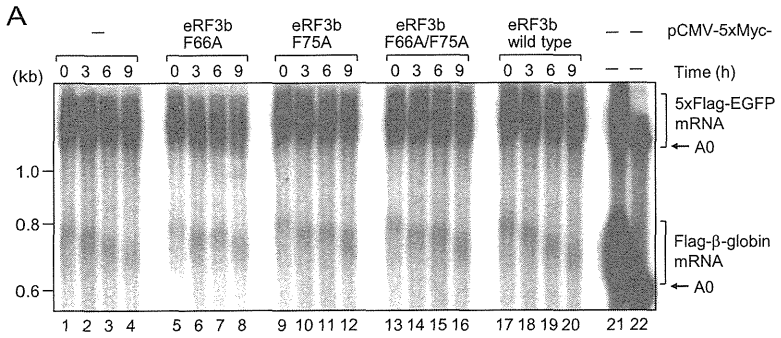

B

pCMV-5xMyc	Deadenylation rate (nt/h)	mRNA Half life (h)
–	13.6 ± 1.7	9.6 ± 1.8
eRF3b F66A	8.0 ± 2.5 *	>17 *
eRF3b F75A	6.8 ± 1.0 *	>17 *
eRF3b F66A/F75A	5.9 ± 0.9 *	>17 *
eRF3b wild type	15.4 ± 2.7	8.7 ± 1.0

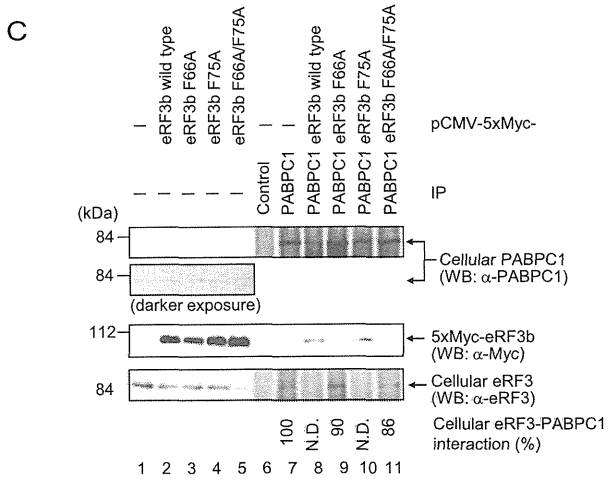

FIGURE 2. Comparison of deadenylation rates and mRNA half-lives in HeLa cells. (*A*) Flag-β-globin and 5xFlag-EGFP mRNAs were analyzed by Northern blotting. HeLa cells were cotransfected with pFlag-CMV5/TO-Gl, pCMV-5xFlag-EGFP, pcDNA6-T7-TR, and either pCMV-5xMyc (lanes *1–4*), pCMV-5xMyc-eRF3b (F66A) (lanes *5–8*), pCMV-5xMyc-eRF3b (F75A) (lanes *9–12*), pCMV-5xMyc-eRF3b (F66A/F75A) (lanes *13–16*), or pCMV-5xMyc-eRF3b (lanes *17–20*). One day later, Flag-β-globin mRNA was induced by tetracycline for 2.5 h, and cells were harvested at the specified times transcription was stopped. To analyze steady-state mRNAs, Flag-β-globin transcription was induced by treatment with tetracycline for 12 h (lanes *21,22*). To mark deadenylated (A0) RNA, the steady-state mRNAs were digested with RNase H in the presence of oligo(dT) (lane *22*). 5xFlag-EGFP mRNA served as a loading control. (*B*) Deadenylation rates and mRNA half-lives were calculated. (*) $P < 0.05$ compared with cells transfected with pCMV-5xMyc. The results in panel *B* are expressed as means ± SD of data from three independent experiments. (*C*) HeLa cells were transfected with pCMV-5xMyc (lanes *1,6,7*), pCMV-5xMyc-eRF3b (lanes *2,8*), pCMV-5xMyc-eRF3b (F66A) (lanes *3,9*), pCMV-5xMyc-eRF3b (F75A) (lanes *4,10*), or pCMV-5xMyc-eRF3b (F66A/F75A) (lanes *5,11*). Cytoplasmic extracts were immunoprecipitated (IP) using anti-PABPC1 (lanes *7–11*) or, as a control, preimmune serum (lane *6*). The immunoprecipitates (lanes *6–11*) and inputs (lanes *1–5*) were analyzed by Western blotting using anti-PABPC1, anti-Myc, or anti-eRF3. Numbers immediately *below* the panel represent IP efficiencies of cellular eRF3 normalized to cellular PABPC1, where the normalized efficiency of cellular eRF3 calculated from lane *7* was defined as 100%. (N.D.) Indicates that cellular eRF3 was not detected. Results are representative of two independent experiments.

which contain PAM2-N and PAM2-C, respectively. ^{1}H–^{15}N HSQC spectra of ^{15}N-labeled PABC showed sharp PABC signals when complexed with either eRF3a(64–82) or eRF3a(73–94), while significant line broadening was observed for ^{15}N-labeled PABC upon addition of increasing amounts of eRF3a(64–94), which contains the two overlapping PAM2 motifs. The broadened signals observed for ^{15}N-labeled PABC–eRF3a(64–94) exist midway between the corresponding signals in the spectra of ^{15}N-labeled PABC in complex with eRF3a(64–82) and eRF3a(73–94) (L585, E601, and E621) (Fig. 5A). There are also signals split into two peaks, each of which overlaps with the corresponding signals in complex with eRF3a(64–82) and eRF3a(73–94) (S591, V607, and Q608) (Fig. 5A). The assignments of these broadened or split signals were confirmed by tracing the signals through titration experiments (Fig. 5B).

It is well known that broadening or splitting of NMR signals is observed in residues experiencing chemical exchange between two states, where the exchange rate is comparable to or slower than the chemical shift difference between states (Cavanagh et al. 2006). Therefore, our NMR results strongly suggest chemical exchange between two complexes: the PAM2-N-bound PABC and the PAM2-C-bound PABC (Fig. 5C). One of the split signals that corresponds to those in complex with eRF3a(64–82) is about twofold stronger than counterparts derived from the complex with eRF3a(79–94), which is consistent with the ITC findings in which eRF3a(64–82) possessed higher affinity for PABC than eRF3a(79–94). At the experimental concentration of 300 μM for PABC and eRF3, the K_d value of 0.4 μM (Table 1) suggests that 96% of the PABC molecules are in the eRF3-bound state. Thus, populations of PABC in the free state and PABC in complex with PAM2-N or PAM2-C are ~4%, 64%, and 32%, respectively.

The ^{1}H chemical shift differences of ^{15}N-labeled PABC in complex with eRF3a(64–82) and eRF3a(73–94) for the broadened residues (e.g., E564,